Mcl1, DNA polymerase α accessory factor, is required for two distinct domain structures in fission yeast centromere

2006 Doctor Thesis

Department of Genetics

School of Life Science

Graduate University for Advanced Studies (Sokendai)

Toyoaki Natsume

January, 2006

Contents

Abstract

Specific chromatin structures on each chromosome location are important for a variety of cellular processes such as transcriptional regulation and chromosome segregation. Although these structures must be precisely maintained during DNA replication to inherit epigenetic information to daughter cells, its underlying mechanisms are poorly understood. In this study, I demonstrate that DNA polymerase α accessory factor, Mcl1, is required for maintaining specific chromatin structures of complex centromere in fission yeast. Fission yeast centromere is composed of two structurally and functionally distinct two chromatin domains. The central domain organizes kinetochore with multiple protein complexes including histone H3 variant, SpCENP-A, and is essential for bipolar attachment to mitotic spindle microtubules from opposite poles. On the other hand, outer repetitive domain forms transcriptionally silent heterochromatin-like structure coated with Heterochromatin Protein 1 (HP1)-homologue, Swi6, and is required for recruiting cohesin complex to tightly bind sister-chromatids. I have shown that Mcl1-deficient cells show alleviation of transcriptional gene silencing of marker genes inserted into both domains. In addition, N-terminal tail of histone H4 is aberrantly acetylated at both domains compared to wild-type strain. At the central domain, SpCENP-A association is abolished in S-phase and the chromatin structure specific to kinetochore is disrupted in Mcl1-deficient cells. At outer repetitive domain, Mcl1 is dispensable for Swi6 loading, suggesting its involvement in an HP1/Swi6-independent pathway for maintaining integrity of heterochromatin. I propose that Mcl1 might maintain histone acetylation pattern suitable for centromeric chromatin structures during DNA replication. This study would provide a novel insight into the close link between DNA replication apparatus and histone acetylation state in the epigenetic inheritance of chromatin structures.

Introduction

Centromere is essential for faithful chromosome segregation and genome stability by serving sites for bipolar attachment to mitotic spindle and for sister chromatid cohesion. Despite its importance for cell viability, DNA sequences of centromere are poorly conserved among eukaryotes. In *Saccharomyces cerevisiae*, a minimum sequence for its function is only 125-bp whereas about 500-kb of highly repetitive sequences composed of 171-bp α-satellite are required in human (Cottarel et al., 1989; Schueler et al., 2001). Overall structures and proteins that constitute centromere, however, are known to be similar in many organisms including fission yeast *Schizosaccharomyces pombe*. Centromere in fission yeast is composed of structurally and functionally distinct two domains, central domain and outer repetitive domain. The central domain consists of central core (*cnt*) and inner part of the inner most repeats (*imr*) sequences, and constructs kinetochore with a variety of conserved proteins such as histone H3 variant, SpCENP-A (Takahashi et al., 2000), while the outer repetitive domain is composed of outer part of *imr* and outer repeat (*otr*) sequences, and forms transcriptionally inactive heterochromatin-like domain, which is coated with *Drosophila melanogaster* Heterochromatin Protein 1 (HP1) homologue, Swi6 (Ekwall et al., 1995; Lorentz et al., 1994). This structural feature that kinetochore is flanked by repetitive heterochromatic element resembles those of metazoan centromeres, making genetically tractable fission yeast an excellent model system to study centromere. The boundary between two domains is defined by tRNA genes that reside on *imr* (Partridge et al., 2000). Both of these domains are indispensable for complete function of centromere (Chikashige et al., 1989; Clarke and Baum, 1990; Hahnenberger et al., 1991; Niwa et al., 1989).

Nucleosomes at the central domain contain SpCENP-A instead of canonical histone H3, and form a specialized chromatin structure, which is considered to be important for centromere function (Marschall and Clarke, 1995; Polizzi and Clarke, 1991; Takahashi et al., 1992). In the conditional mutant of SpCENP-A (*cnp1-1*), fatal unequal chromosome segregation is observed and the specialized chromatin structure is disrupted (Takahashi et al., 2000). It has been recently suggested that at least two pathways are responsible for SpCENP-A loading in fission yeast: Mis6 pathway and Ams2 pathway (Takahashi et al., 2005). Mis6 was identified in a screening for mutants that frequently lose mini-chromosome and show unequal segregation at the restrictive temperature (Takahashi et al., 1994). Although precise function of this gene product remains unclear, its homologues are conserved in many organisms, such as Ctf3 in *S. cerevisiae* (Measday et al., 2002) and CENP-I in vertebrates (Nishihashi et al., 2002). Mis6 constitutively localizes to the central domain and is required for SpCENP-A loading possibly at S phase and G2 phase (Takahashi et al., 2000; Takahashi et al., 2005). Mis6 forms a complex with Mis15, Mis17, and Sim4, and their localization to the central domain is mutually dependent (Hayashi et al., 2004; Pidoux et al., 2003). Binding of Mis6 to the central domain also depends on Mis16 and Mis18 (Hayashi et al., 2004). Interestingly, Mis16 is quite similar to human retinoblastoma-associated protein, RbAp46 and RbAp48 (also known as CAF-1 p48 subunit, Verreault et al., 1996), which are found in two distinct histone deacetylase (HDAC) complexes, called Sin3 complex (Zhang et al., 1997) and NuRD (nucleosome remodeling histone deacetylase) complex (Tong et al., 1998; Xue et al., 1998; Zhang et al., 1998). In agreement with these facts, histone H4 at the central domain is highly acetylated in the conditional mutant of *mis16*, suggesting that hypoacetylated state of histone H4 is required for efficient SpCENP-A loading. On

the other hand, Ams2 is a cell cycle-regulated GATA factor that binds to the central domain from G1/S to early G2 phase, and is believed to be required for SpCENP-A loading at S phase (Chen et al., 2003). The *ams2*$^{+}$ gene was isolated in a screening that searches for multi-copy suppressor of *cnp1-1* mutant, and in this screening, the gene that codes histone H4 was also isolated. The *ams2Δ* mutant is viable, but shows severe growth defect accompanying with chromosome missegeregation. In the *ams2Δ* mutant, periodical expression of histone genes is abolished, indicating that enough amounts of histones are required for SpCENP-A loading. In addition, Chen et al. suggested that Ams2 might directly function at the central domain because binding of vertebrate GATA factors to chromatin stimulate chromatin remodeling (Boyes et al., 1998; Chen et al., 2003; Cirillo et al., 2002). Interestingly, the human NuRD HDAC complex mentioned above also contains SWI/SNF-related chromatin remodeling factor, CHD3 and CHD4 (chromo-ATPase/helicase-DNA binding domain) proteins (Tong et al., 1998; Xue et al., 1998; Zhang et al., 1998), and fission yeast genome codes two genes that belong to this family, *hrp1*$^{+}$ and *hrp3*$^{+}$. The *hrp1Δ* mutant shows inefficient SpCENP-A loading and increased acetylation of histone H4 at the central domain, and Hrp1 is assigned to Ams2 pathway (Walfridsson et al., 2005), suggesting that chromatin remodeling (Ams2 and Hrp1) and histone deacetylation (Mis16) might be closely related.

On fission yeast chromosomes, heterochromatic regions are found at outer repetitive domain of centromere, mating type (*mat*) loci, telomere, and ribosomal DNA cluster (Cam et al., 2005). These regions show transcriptionally silent state as marker genes inserted there are repressed (Allshire et al., 1995). At these regions, Suv39h methyltransferase homologue, Clr4, adds methyl-residues to histone H3-K9, to which HP1/Swi6 selectively binds through its chromo-domain (Nakayama et al., 2001b). In

addition, N-termini of histone H3 and H4 are hypoacetylated, and this state is also important for heterochromatin assembly. For example, transient treatment with histone deacetylase inhibitor, Trichostatin A (TSA) disrupts centromere function (Ekwall et al., 1997). Among members coded in the fission yeast genome, four HDACs are shown to be required for heterochromatin assembly. NAD^+-dependent HDAC, Sir2, is required for deacetylation of H3-K9, which is prerequisite for subsequent methylation of same residue (Shankaranarayana et al., 2003). Another *SIR2* family HDAC, Hst4 is involved in centromeric and telomeric heterochromatin (Freeman-Cook et al., 1999). Clr3 and Clr6 HDACs deacetylate H3-K14 and broad substrates *in vivo*, respectively, and both of them are required for heterochromatin assembly at centromere and *mat* loci (Grewal et al., 1998; Nakayama et al., 2003; Silverstein et al., 2003; Yamada et al., 2005). Recently, RNA interference (RNAi) machinery and small interfering RNA (siRNA) were shown to be required for targeting of heterochromatin (Hall et al., 2002; Sugiyama et al., 2005; Verdel et al., 2004; Volpe et al., 2002). First, RNAs transcripted from outer repeats of centromere (*dg*) change into double strand RNA (dsRNA) by the action of RNA-dependent RNA polymerase (RdRP), and RISC (RNA-induced silencing complex) processes the dsRNA into siRNA, which in turn forms a complex with RITS (RNA-induced initiation of transcriptional gene silencing) that contains chromo-domain protein, Chp1. Next, RITS is targeted to homologous sequences corresponding to siRNA and recruits Clr4, which makes a binding site for Swi6. These discoveries solved a question that “How is heterochromatin established at a specific site?” Once established, the epigenetic state must be inherited during proliferation. In spite of great progress in understanding establishment step, mechanism of maintenance step during DNA replication is poorly understood. Two groups have reported, however, that a catalytic

subunit of DNA polymerase α in fission yeast, Swi7, is required for Swi6 loading onto heterochromatin including outer centromere (Ahmed et al., 2001; Nakayama et al., 2001a), providing a direct link between DNA replication and maintenance of heterochromatin during DNA replication.

In an effort to isolate novel genes involved in recombinational repair, the *slr3-1* (*mcl1-101*) was isolated as a mutation that is synthetically lethal with a mutation of the *rad2*$^+$ gene, which is involved in Okazaki fragment processing (Tsutsui et al., 2005). In parallel, Williams and McIntosh isolated the identical gene by screening for mutants that frequently lose mini-chromosome and designated this gene as *mcl1*$^+$ (mini chromosome loss) (Williams and McIntosh, 2002). The null mutant of *mcl1*$^+$ gene is lethal (Williams and McIntosh, 2002), or sick (Tsutsui et al., 2005), suggesting that the *mcl1*$^+$ gene is important for cell growth. The *mcl1-101* mutant is moderately sensitive to DNA damaging agents, such as MMS and gamma-rays, and is temperature sensitive for growth. In addition, *mcl1-101* shows synthetic lethality and severe growth defect with the mutation of *dna2*$^+$, a helicase involved in Okazaki fragment processing, and the mutation of *swi7*$^+$, respectively. Furthermore Mcl1 physically interacts with Swi7 *in vivo* and *in vitro*. These results suggested that *mcl1*$^+$ is involved in lagging strand DNA synthesis (Tsutsui et al., 2005). Mcl1 is well conserved from yeast to human, and this family of proteins contain WD40 repeats domain at its N-terminus, which is known to mediate protein-protein interaction (Smith et al., 1999), and SepB box at its C terminus, whose function is unknown. The *S. cerevisiae* homologue *CTF4* was isolated by two groups as a gene which is required for chromosome stability (Kouprina et al., 1993) or which physically interacts with Pol1, a catalytic subunit of DNA polymerase α in *S. cerevisiae* (Miles and Formosa, 1992). The Ctf4 is believed to function in the establishment of sister

chromatid cohesion (Hanna et al., 2001). In agreement with this, truncated alleles of *mcl1*$^{+}$ gene, *mcl1-1* (Williams and McIntosh, 2002) and *mcl1-102* (Tsutsui et al., 2005) show a defect in sister-chromatid cohesion near centromere and synthetic lethality with a conditional mutant of *rad21*$^{+}$, which codes a component of cohesin complex (Williams and McIntosh, 2002; Y. Tsutsui, unpublished data).

In fission yeast, cohesin is known to be preferentially enriched at outer repetitive centromere in Swi6-dependent manner (Bernard et al., 2001; Nonaka et al., 2002). As described above, loading of Swi6 onto this region requires DNA polymerase α catalytic subunit, Swi7 (Ahmed et al., 2001; Nakayama et al., 2001a). Furthermore, Mcl1 physically interacts with Swi7 (Tsutsui et al., 2005; Williams and McIntosh, 2005). Taken together, I hypothesized that Mcl1 might be directly involved in heterochromatin assembly in concert with Swi7 (that is, Swi6 loading), and contribute to sister chromatid cohesion at outer centromere indirectly.

In this study, based on this hypothesis, I have analyzed roles of Mcl1 in chromosome metabolism. I have shown that Mcl1 is required for the maintenance of heterochromatin at outer centromere as well as *mat* loci and telomere. However, in contrast to Swi7, Mcl1 acts on outer centromeric heterochromatin independent of Swi6. I have also demonstrated that Mcl1 is essential for the central domain structure of centromere. The *mcl1* mutant is deficient in SpCENP-A association to the central domain during S-phase. In addition, acetylation of histone H4 is elevated at the central domain as well as outer centromeric heterochromatic domain in the *mcl1-101* mutant. Thus I have concluded that Mcl1 has important roles in two distinct chromatin structures of fission yeast centromere by maintaining hypoacetylated state of histone H4. This study has shed light on the epigenetic inheritance of chromatin structures during DNA replication.

Materials and Methods

Strains, plasmids, and drug sensitivity tests. *S. pombe* strains used in this study are listed in Table 1. *S. pombe* cells were routinely grown in YES (complete media) and EMM (minimum media) supplemented with appropriate nutrients. Mating and sporulation were induced on SPA media supplemented with appropriate nutrients. Standard genetic manipulations are used as previously described (Moreno et al., 1991). The *chp1*$^{+}$ and *mis6*$^{+}$ genes were C-terminally tagged with GFP, and *rad21*$^{+}$ with Myc, respectively, at the endogenous loci using PCR-based tagging module (Bahler et al., 1998). The SpCENP-A gene (*cnp1*$^{+}$) was C-terminally tagged with 3x FLAG and 6x His at the endogenous locus using pFA6a-FH-kanMX6, which was constructed using PCR-based tagging module (a gift from Dr. T. Morishita). The pREP41 (Basi et al., 1993) is an autonomously-replicating multi-copy plasmid and carries *S. cerevisiae LEU2* gene, an autonomously replicating sequence, *ars1*, and middle strength thiamine-repressible *nmt41* promoter. Plasmids pREP41-EYFP and pREP41-EGFP were constructed by inserting genes that code EYFP (Clontech) and EGFP into the multi-cloning site of pREP41, respectively (gifts from Dr. H. Iwasaki). The multi-copy plasmid pSP102 carries the *LEU2* gene and an autonomously replicating sequence, *ars2004* (Okuno et al., 1997), and used for overexpression of SpCENP-A and Mcl1 (a gift from Dr. H. Masukata). Sensitivity to drugs were examined by plating ten-fold dilutions of *S. pombe* cells onto YES containing 10 – 20 μg/ml of TBZ (Sigma) or 10 – 25 μg/ml of TSA (Wako), or streaking cells onto YES containing 10 mM hydroxy urea (HU), and plates were incubated for 3 days.

Quantitative reverse transcription (RT) –PCR. Total RNA was extracted from log-phase cells using RNeasy Mini Kit (Qiagen) and treated with DNase I (Takara) to digest contaminated genomic DNA. RT reaction was performed with oligo-dT primer using Perfect Real time RT-PCR Kit (Takara). Real-time PCR was carried out using SYBR Premix Ex Taq (Takara) and LightCycler (Roche). The nucleotide sequences of primers used are listed in Table 2.

Western blotting. Total protein extracts for western blotting were prepared as previously described (Kaiser et al., 1994) with some modifications. Approximately 4 x 10^7 log-phase cells were resuspended in 30 μl of 1x SDS Loading Buffer (50 mM Tris-HCl pH 6.8, 2% SDS, 10% glycerol, 0.1% bromophenol blue, 10% 2-mercaptoetanol) and boiled for 3 min. The cell suspension was vigorously shaken with 0.1 g of glass beads (Sigma) by vortexing for 10 min. The suspension was mixed with additional 70 μl of 1x SDS Loading Buffer and boiled for 3 min. Two-fold dilutions of the protein extracts were separated on SDS gel and blotted onto Hybond-P (Amersham). Proteins were detected by α-acetyl histone H4 (2-19) antiserum (Upstate, #06-866) or α-Cdc2 /PSTAIRE (Santa Cruz, #sc-53) using horseradish peroxidase-conjugated secondary antibodies (Amersham) and ECL Plus Western Blotting Detection Reagents (Amersham).

Fluorescent microscopy. For observation of nucleus, cells were stained by fixing with 70% EtOH and adding 1 μg/ml of 4', 6-Diamidino-2-phenylindole, dihydrochloride (DAPI), and were observed under ECLIPSE E800 (Nikon). For examination of Swi6-EYFP localization, strains carrying *swi6*$^+$ gene that was C-terminally tagged with EYFP at the endogenous locus (a gift from Dr. H. Iwasaki) was

observed under FV1000 laser confocal microscope (Olympus) or DeltaVision (Applied Precision). For examining co-localization of Swi6-EYFP and EGFP-SpCENP-A, pREP41-EGFP-*cnp1*$^{+}$ was introduced into *swi6*$^{+}$*-EYFP* strains, and cells were observed under inducible condition (-thiamine) using FV1000 laser confocal microscope (Olympus). For observation of EYFP-SpCENP-A, pREP41-EYFP-*cnp1*$^{+}$ was introduced and cells were observed under inducible condition using ECLIPSE E800 (Nikon).

Chromatin immunoprecipitation (ChIP) assay. ChIP assay was performed as described previously with some modifications (Ekwall and Partridge, 1999). Approximately 4 x 10^{8} log-phase cells per each reaction, grown in YES at the temperature described in the text, were fixed by adding 1/10 volume of the fixation solution (30% formaldehyde, 0.3N NaOH). Fixation was performed with gentle agitation at the same temperature as previous incubation for 5 min, on ice for 3min, and at 18 ºC for 22 min. Fixation was stopped by adding 1/20 volume of 2.5 M glycine. Fixed cells were washed twice with ice-cold DW and stored at -80 ºC. Following reactions were performed at 4 ºC or on-ice. Cells were resuspended in a 1.5 ml screw-tube with 300 μl of ice-cold Lysis Buffer (50 mM HEPES-KOH pH 7.5, 140 mM NaCl, 1 mM EDTA, 1% Triton X-100, 0.1% sodium deoxycholate) containing 1x protease inhibitor cocktail (Pierce) and lysed with 3 or 4 x 5 min pulses on the bead beater, MicroSmash (Tomy) using 710-1,180 μm glass beads (Sigma). The base of the 1.5 ml tube was punctuated with a needle and it was placed on a 1.5 ml eppendolf tube, and centrifuged at 5,000 rpm for 1 min to spin the cell lysate into the 1.5 ml eppendolf tube. The pellet was resuspended by pipetting and sonicated with 1 min x 6 pulses at maximum power using

Bioruptor (CosmoBio) to shear the chromatin to ~500 bp. Efficiency of the sonication was confirmed later by polyacrylamide gel electrophoresis. The lysate was centrifuged at 15,000 rpm for 5 min and the supernatant was transferred to a new 1.5 ml eppendorf tube. Again the lysate was centrifuged for 10 min and the supernatant was transferred to a new tube. For IP sample, 500 μl of the lysate was mixed with 20 μl of Protein A Magnetic Beads (New England Biolabs) or Dynabeads Protein A (Dynal Biotech) pre-washed with Lysis Buffer, and incubated with rocking for 1 hr to reduce non-specific binding to the beads. The beads were precipitated by magnetic force using a special rack, and the supernatant was transferred to a new 1.5 ml eppendolf tube. The lysate was mixed with 5 μl of monoclonal α-GFP antibody JL-8 (Clontech, #8371-2), 10 μl of polyclonal α-c-Myc antibody (Santa Cruz, sc-789), or 5 μl of α-acetyl histone H4 antiserum (Upstate, #06-866) and incubated for over night with rocking. As a negative control sample, same procedures were performed using 250 μl of the lysate except for without adding the antibody. For input sample, 50 μl of the lysate was mixed with 200 μl of TES (50 mM Tris-HCl pH 8.0, 10 mM EDTA, 1% SDS) and incubated at 65 ºC for at least 6 hr to reverse cross-linking. The lysate/antibody was mixed with 20 μl of Protein A Magnetic Beads or Dynabeads Protein A, and incubated for 1 hr with rocking. The beads was precipitated with the rack, and washed with 1 ml of following solutions: Lysis Buffer x 2, Wash Buffer I (50 mM HEPES-KOH pH 7.5, 500 mM NaCl, 1 mM EDTA, 1% Triton X-100, 0.1% sodium deoxycholate) x 1, Wash Buffer II (10 mM Tris-HCl pH 8.0, 250 mM LiCl, 0.5% NP-40, 1 mM EDTA, 0.5% sodium deoxycholate) x 1, and TE (10 mM Tris-HCl, 1 mM EDTA) x 2. After residual TE in the tube was completely removed, the beads was resuspended in 50 μl of TES, mixed by vortex, and incubated at 65 ºC for 10 min to elute DNA/Protein complex from the beads. The beads was precipitated by the rack and

the elution was transferred to a new 1.5 ml eppendorf tube. Again, the beads was resuspended in 200 μl of TES, mixed by vortex, and incubated at 65 ºC for 5 min. After precipitation, the elution was mixed together with previous 50 μl, and incubated at 65 ºC for at least 6 hr to reverse cross-linking. The elution was mixed with 250 μl of TE and 12.5 μl of Proteinase K (Roche), and incubated at 37 ºC for 2 hr. Immunoprecipitated DNA was extracted with phenol/chloroform and chloroform, and then EtOH-precipitated by adding 2.5 volume of 99.5% EtOH and 1/10 volume of 3M NaOAc (pH 5.2). The pellet was resuspended in 100 μl of TE (pH 8.0) containing 10 μg/ml of RNase A and incubated at 37 ºC for 20 min. Same procedures were performed for the negative control sample (1/2x scale) and the input sample (1x scale). Quantification of immunoprecipitated DNA was performed by real-time PCR using SYBR Premix Ex Taq (Takara) and LightCycler (Roche) following manufacture's instructions. The nucleotide sequences of primers used in real-time PCR are listed in Table 2.

Micrococcal nuclease (MNase) assay. MNase assay was performed as described previously with some modifications (Pidoux et al., 2004). Approximately 1.5 x 10^9 log-phase cells, incubated at 36 ºC for 6 hr prior to collection, were resuspended in 20 ml of SP1 (20 mM phosphate/citrate pH 5.6, 40 mM EDTA) containing 40 μl of 2-mercaptoetanol and incubated at RT for 10 min. The cell was precipitated and resuspended in SP2 (50 mM phosphate/citrate pH 5.6, 1.2M sorbitol) containing 2 mg/ml of Zymolyase 100T (ICN) and incubated at 36 ºC for 15 min with vigorous shaking to partially digest the cell wall. The spheroplast was washed three times with 20 ml of SP3 (10 mM Tris-HCl pH 7.6, 1.2 M sorbitol) by gentle pipetting, and resuspended in 10 ml

of NDB (10 mM Tris-HCl pH 7.5, 1.2 M sorbitol, 50 mM NaCl, 5 mM $MgCl_2$, 1 mM $CaCl_2$). The spheroplast was precipitated, resuspended in 1.6 ml of NDB-BS (15 ml of NDB, 1 μl of 2-ME and 7.5 μl of 1M spermidine·3HCl), divided into 200 μl aliquots and pre-warmed at 36 ºC. The spheroplast was mixed with 200 μl of pre-warmed MNase (Worthington Biochemical) diluted at 0, 25, 50, 100, 200, 300 and 500 U/ml in NDB-BS containing 0.15% NP-40 and incubated at 36 ºC for 20 min to digest the genomic DNA. The spheroplast/MNase was mixed with 40 μl of pre-warmed STOP solution (250 mM EDTA, 5% SDS) to terminate the reaction, mixed with 3 μl of proteinase K (Roche) and incubated at 50 ºC for over night. Digested DNA was extracted with phenol/chloroform and chloroform ,and EtOH-precipitated. Precipitated DNA was resuspended in 30 μl of TE (pH 8.0) containing 100 μg/ml of RNase A and incubated at 37 ºC for 1hr. MNase-digested samples were separated on 1.5% agarose gel and analyzed by Southern hybridization using AlkPhos Direct Labelling and Detection System (Amersham). The nucleotide sequences of primers used for amplifying probe DNA are listed in Table 2.

Results

The *mcl1-101* mutant cell shows aberrant mitosis. Defect in sister chromatid cohesion results in premature separation of sister centromeres, which is frequently observed in cells harboring the *mcl1-1* mutation (Williams and McIntosh, 2002) that terminates at 124th codon of Mcl1 protein (815 amino acid), and the *mcl1-102* mutation (Tsutsui et al., 2005) that codes 1-268th amino acid and 11-unrelated C-terminal residues. Indeed, the *mcl1-1* mutant shows aberrant mitosis such as lagging chromosome, indicative of impaired sister chromatid cohesion, and unequal chromosome segregation (Williams and McIntosh, 2002). Another allele, the *mcl1-101* mutation causes temperature sensitivity for growth and has three point mutations at its C-terminal half, and results in Pro to Ser (493th), Leu to Phe (763th), and Ala to Val (768th) amino acid changes (Tsutsui et al., 2005). To examine mitotic phenotype of this mutant, *mcl1-101* cells were grown at 37 ºC for 6 hr before fixation and treatment with DAPI. Some portion of *mcl1-101* mutant cells showed unequal chromosome separation (Fig. 1A, arrows). The *mcl1Δ* mutant cell also showed unequal chromosome separation as well as lagging chromosomes (Fig. 1A), and the frequency of aberrant mitosis was higher than that in *mcl1-101* cells. This result indicates that *mcl1-101* mutant is defective in mitosis at the restrictive temperature, but it is relatively moderate compared to the null mutation. Although lagging chromosome was not detected in *mcl1-101* cells, the *mcl1-101* mutation was synthetic lethal with a conditional mutation of the *rad21*$^{+}$ gene, which encodes a non-SMC subunit of cohesin complex (Table 3), suggesting that *mcl1-101* cells also have a defect in sister chromatid cohesion, which produces lagging chromosomes. Since *mcl1Δ* and *mcl1-102* mutants cells show severe growth delay, the *mcl1-101* mutant

was used in the following experiments.

Genetic interaction between Mcl1 and DNA polymerase α, Swi7. In fission yeast, it was reported that loading of Swi6 onto heterochromatin requires DNA polymerase α catalytic subunit, Swi7 (Ahmed et al., 2001; Nakayama et al., 2001a). The *mcl1-101* mutant shows a slight reduction in its permissive growth temperature when combined with a mutation of the *swi7*$^{+}$ gene, *polα ts13* (Tsutsui et al., 2005), but this mutation does not show any defect in heterochromatin (Y. Tsutsui, unpublished result). To further analyze the relationship between Mcl1 and Swi7, I examined genetic interactions with other *swi7* alleles, *swi7-1* and *swi7-H4*, both of which were reported to be defective in the maintenance of heterochromatin (Fig. 1B). The *mcl1-101 swi7-H4* double mutant was viable, but showed an exceedingly reduced temperature for growth (Fig. 1C and Table 3) and showed an extremely elongated morphology at 30 ºC, which was similar to that of the *mcl1-101* single mutant cell at the restrictive temperature, 37 ºC (data not shown). The *swi7-1* mutation was synthetically lethal with the *mcl1-101* mutation even at 25 ºC (Fig. 1D and Table 3). These results suggest that Mcl1 and Swi7 have a functional link in chromatin regulation, and that Mcl1 might be also required for Swi6 loading as Swi7. Cohesin is known to be preferentially enriched at the outer centromere in Swi6-dependent manner (Bernard et al., 2001; Nonaka et al., 2002). As sister chromatid cohesion near centromere is compromised in *mcl1* mutants (Williams and McIntosh, 2002; Y. Tsutsui, unpublished result), I hypothesized that Mcl1 might be directly involved in the maintenance of heterochromatin in concert with Swi7 (that is, Swi6 loading), and contribute to sister chromatid cohesion at outer centromere indirectly.

Transcriptional gene silencing is alleviated in the *mcl1* mutant. To assess maintenance of heterochromatin in the *mcl1* mutant, we used three indicator strains as follows: FY1193 strain that harbors both *ura4*$^+$ gene (pyrimidine base biosynthesis) and *ade6*$^+$ gene (purine base metabolism) inserted into outer centromere (outer part of *imr* and *otr*) on centromere I (Allshire et al., 1995), FY597 strain that carries the *ura4*$^+$ gene inserted into centromere-distal side of *mat3M* loci (Allshire et al., 1995), and FY520 strain that harbors the *ura4*$^+$ gene adjacent to telomere on the non-essential mini-chromosome (Nimmo et al., 1994) (Fig. 2A-C). These marker genes inserted into heterochromatin are transcriptionally repressed, and this phenomenon is called transcriptional gene silencing (TGS). TGS can be used as an indicator of heterochromatin function since its alleviation is observed in mutants defective in heterochromatin assembly (Allshire et al., 1994; Allshire et al., 1995). TGS of these strains were assayed on EMM plates containing 5-FOA, which kills *ura4*$^+$-expressing cells, and on YE plates, which contains low concentration of adenine and changes colony color of *ade6*$^+$-expressing cells from red to white. The *mcl1-101* mutant harboring maker genes at outer centromere was more sensitive to 5-FOA and became pink on the low adenine plate compared to the wild-type (*wt*) strain (Fig. 2A). The level of alleviation in *mcl1-101* cells was comparable to that of *swi6Δ* cells at *imr* (FOA), but not at *otr* (Low adenine) in which *swi6Δ* cells showed more severe de-repression. In addition, *mcl1-101* cells also showed a defect in TGS at *mat* loci (Fig. 2B) and slightly at telomere (Fig. 2C). In agreement with previous reports, *swi7-H4* and *swi7-1* cells also showed alleviation of TGS at heterochromatic regions tested, except for telomere in *swi7-1* cells (Fig. 2A-C and data not shown). To confirm whether transcripts from heterochromatic regions are indeed increased, quantitative RT-PCR for the *ura4*$^+$ gene inserted into *imr* was

performed. While *swi6Δ* and *clr4Δ* mutants accumulated 5.8- and 18.1-fold *ura4*$^+$ transcripts compared to the *wt* strain, 2-fold increase in the transcripts was detected in the *mcl1-101* mutant at the semi-permissive temperature, 32 ºC (Fig. 2D). These results suggest that Mcl1 is involved in the maintenance of heterochromatin at three regions, possibly in concert with Swi7.

The role of Mcl1 in the maintenance of heterochromatin is unique among DNA replication apparatus. It is possible that alleviation of TGS observed in *mcl1-101* and *swi7* mutants might be an indirect consequence resulting from destabilized replication fork. To eliminate this possibility, TGS was examined in other replication-related mutants (Fig. 3A). The *polδ ts02* is a conditional mutation of a catalytic subunit of DNA polymerase δ, which is considered to have central roles in chromosomal DNA replication, DNA repair, and recombination (Hubscher et al., 2000). Both *rad2*$^+$ and *dna2*$^+$ genes code nucleases involved in Okazaki fragment processing. None of these mutants showed a defect in TGS at outer centromere (Fig. 3A). Furthermore, the null mutant of DNA replication-checkpoint gene, *rad3*$^+$, also did not show any alleviation of TGS at outer centromere (Fig. 3B). These results suggest that Mcl1 and Swi7 have a unique function among DNA replication machinery in the maintenance of heterochromatin.

Centromeric heterochromatin does not depend on integrity of sister chromatid cohesion. Next, TGS at outer centromere was examined in mutants deficient in sister chromatid cohesion. The *eso1*$^+$ gene was shown to be required for the establishment of sister chromatid cohesion during S-phase (Tanaka et al., 2000). The *ctf18*$^+$ gene is homologous to *S. cerevisiae CTF18*, which forms an alternative RFC

complex, and is also required for the establishment of sister chromatid cohesion (Mayer et al., 2001). The *ctf18Δ* mutant was viable, but showed increased mini-chromosome loss frequency (Y. Tsutsui, unpublished result). None of these mutants showed a defect in TGS at outer centromere (Fig. 3A). It was reported that a mutation of the *psc3*$^{+}$ gene, which encodes a non-SMC subunit of cohesin complex, shows no defect in TGS at outer centromere (Nonaka et al., 2002). These results support the idea that sister chromatid cohesion at outer centromere depends on centromeric heterochromatin, but not vise versa. Therefore Mcl1 might have a direct function in the maintenance of heterochromatin, which is essential for sister chromatid cohesion at outer centromere.

Endogenously repressed *mat2P* gene at *mat* loci is aberrantly expressed in the *mcl1-101* mutant. *S. pombe mat* loci are composed of expressed *mat1P/M* locus and silent *mat2P* and *mat3M* loci, and information of *mat1* locus (P or M) is switched by copy transposition (Beach, 1983). At least two pathways are known to redundantly repress the expression from the silent loci: *trans*-acting factors, such as Clr1-4 and Swi6, and *cis*-acting sequences near *mat2P* and *mat3M*. When combined with deletion of the *cis*-acting sequence near *mat2P* (*Bgl*II-*Bss*HII fragment), mutants of *clr1-4*, *swi6*, and *swi7* genes show severe de-repression of *mat2P* gene, resulting in the expression of both mating type genes which leads to aberrant meiosis in haploid cell, that is called “Haploid meiosis” (Ahmed et al., 2001; Nakayama et al., 2001a; Thon et al., 1994). To examine whether Mcl1 is required for repression of the silent loci, *mat2PΔ* (*Bgl*II-*Bss*HII) deletion was introduced into the *mcl1-101* mutant. Haploid meiosis can be easily detected by treating a colony with iodine vapor that stains resultant spores into brown. The *mcl1-101* mutant became light brown after treating with iodine vapor whereas the *wt* strain remained white

and the *swi6Δ* mutant turned dark brown (Fig. 4). This result indicates that Mcl1 is also required for repressing the expression of endogenously silenced *mat* loci.

Microscopic analysis of Swi6 localization to heterochromatic regions in the *mcl1* mutant. Swi6 is an essential component of heterochromatin and constitutively localizes to heterochromatic regions. This localization can be observed by immunostaining as two to four spots in the nucleus, which represent centromere, *mat* loci, and telomeres (Ekwall et al., 1995). In *clr4* mutant cells, Swi6 is delocalized from these regions, and dispersed within the nucleus (Ekwall et al., 1996). To observe Swi6 localization in the *mcl1-101* mutant, the *swi6*$^{+}$*-EYFP* gene was expressed under its own promoter. The *swi6*$^{+}$*-EYFP* strain was not sensitive to microtubule-destabilizing drug, TBZ, and did not show any defect in TGS at outer centromere, indicating that Swi6-EYFP is functional (Y. Akamatsu, personal communication). At the permissive temperature for *mcl1-101* (25 ºC), *wt* and *mcl1-101* cells formed one to four spots in the nucleus while *clr4Δ* cells did not, as reported previously (data not shown). Next, Swi6 localization was observed at the semi-permissive (32 ºC) and the restrictive temperature (37 ºC for 6 hr). As shown in Fig. 5A, in contrast to *wt* cells in which two major spots with some minor spots were observed, *mcl1-101* cells showed only one major spot with several faint spots at both temperatures. To examine which heterochromatic region retains Swi6 in *mcl1-101* cells, N-terminally EGFP tagged SpCENP-A gene (*EGFP-cnp1*$^{+}$) was expressed under *nmt41* promoter as a marker for centromere (Fig. 5B). In the most part of *mcl1-101* cells, EGFP-SpCENP-A localized at 37˚C when overexpressed. The major Swi6-spot remaining in *mcl1-101* cells at 37 ºC coincided with the EGFP-SpCENP-A signal, indicating that *mcl1-101* cells could retain Swi6 to centromere. Another spot that

became faint or disappeared in *mcl1-101* cells is discussed later.

In addition, the *chp1*$^{+}$ gene was endogenously tagged with GFP and its localization was observed in *mcl1-101* cells. Chp1 protein is a component of RITS complex required for targeting (that is, establishment) of heterochromatin to a specific site (Verdel et al., 2004), and also constitutively localizes to heterochromatic regions depending on the action of Clr4 (Sadaie et al., 2004). Chp1-GFP formed one to four spots in *mcl1-101* cells similar to *wt* cells (Fig. S1), indicating that Mcl1 is dispensable for RITS association to heterochromatic regions.

ChIP analysis of Swi6 localization to heterochromatic regions in the *mcl1* mutant. To further analyze localization of Swi6 in the *mcl1-101* mutant, chromatin immunoprecipitation (ChIP) assay was performed using same strains as in Fig. 5A. Precipitated DNA was quantified by real-time PCR using several sets of primers corresponding to heterochromatic regions and euchromatic regions (Fig. 6A). In the *wt* strain, Swi6-EYFP was enriched at heterochromatic regions such as outer centromere (*imr195*, *dg*, and *dh*), *mat* loci (*mat2P* and *cenH*), and telomere (*TEL*) compared to euchromatic regions (*ade6* and actin gene, *act1*) (Fig. 6B). In contrast, association of Swi6-EYFP at heterochromatic regions was abolished in the *clr4Δ* mutant, consistent with previous reports (Nakayama et al., 2001b). In the *mcl1-101* mutant, association of Swi6-EYFP to outer centromere (*imr195*, *dg*, and *dh*) was not impaired, or rather, slightly increased (1.5- to 1.8-fold). In addition, Swi6-EYFP association to the *ura4*$^{+}$ gene inserted into *imr* (Fig. 2A) was not decreased (Fig. S2). Swi6-EYFP enrichment at *mat* loci (*mat2P* and *cenH*) was slightly decreased (0.7-fold at both regions), while that of telomere (*TEL*) was comparable to the *wt* strain. Partial impairment of Swi6-EYFP

association was observed in the *swi7-H4* mutant: 0.59- to 0.65-fold at outer centromere, 0.43- to 0.45-fold at *mat* loci, and 0.71-fold at telomere). These results suggest that Mcl1 is dispensable for Swi6 localization to outer centromere and telomere in contrast to Swi7, but might have a subtle function at *mat* loci.

Mcl1 and Swi7 have a Swi6 independent function at centromere. To further assess the relationship between Mcl1 and Swi6, their genetic interaction was examined using microtubule-destabilizing drug, TBZ. Since mutants deficient in centromeric sister chromatid cohesion (that is, outer centromeric heterochromatin) or kinetochore function are known to be sensitive to TBZ, sensitivity to this drug can be used as an indicator of centromere integrity. The *mcl1-101 swi6Δ* double mutant was constructed and turned out to be viable with a slight slow growth. However, the double mutant showed a synergistic sensitivity to TBZ compared to each single mutant (Fig. 7A and Table 3). These results suggest that Mcl1 has Swi6-independent function in maintaining centromeric heterochromatin, or in other distinct processes. Interestingly, the *swi7-H4* mutant also showed a synergistic interaction with the *swi6Δ* mutation in TBZ sensitivity (Fig. 7A), indicating that Swi7 also might have a novel function at centromere other than Swi6 loading. In consistent with this idea, I found that both *mcl-101* and *swi7* mutants showed a higher sensitivity to TSA, which specifically inhibits HDAC activity (Yoshida et al., 1990) at the concentration of 25 μg/ml, at which neither the *wt* strain nor the *clr4Δ* mutant showed the sensitivity (Fig 7B). It was reported that transient treatment with TSA increased the level of histone acetylation at outer centromere and impaired centromeric heterochromatin (Ekwall et al., 1997). Thus Mcl1 and Swi7 might be implicated in outer centromeric heterochromatin by an HDAC-related process independent of Swi6-Clr4.

Furthermore, preferential centromeric localization of Rad21, a cohesin subunit, was not decreased in the *mcl1-101* mutant in contrast to the *swi6Δ* mutant (Fig. S3), suggesting that Mcl1 has an unknown role in centromeric cohesion distinct from cohesin localization.

Histone H4 at the outer heterochromatic domain and the central domain are hyper-acetylated in the *mcl1* mutant. As *mcl-101* and *swi7* mutants were found to be sensitive to TSA, I examined the acetylation state of histone H4 by ChIP assay using an antiserum against a peptide corresponding to amino acid 2-19 of histone H4 acetylated at K5, K8, K12 and K16. Acetylation at heterochromatic regions was increased by 2.3-fold (*imr-195*), 3.0-fold (*dg-223*), 2.2-fold (*cenH*) and 25-fold (*TEL*) in the *mcl1-101* mutant (Fig. 8B). Acetylation at euchromatic regions was also increased by 1.9-fold (*lys1*) and 1.4-fold (*ade6-2*), but degree of increase was relatively moderate compared to that of other regions. In the *swi7-1* mutant, however, no significant increase was observed in heterochromatic regions. The acetylation level of total histone H4 was not altered in the *mcl-101* mutant (Fig. 8C), indicating that increase in the acetylation is not a global phenomenon.

Unexpectedly, acetylation levels at the central domain were markedly increased in the *mcl1-101* mutant by 4-fold (*cnt-2*) and 5.3-fold (*imr-256*) compared to those in the *wt* strain (Fig. 8B). Increase of acetylation level was also observed in the *swi7-1* mutant at the central domain by 2.2-fold (*cnt-2*). At the central domain, N-terminal tails of histone H3 and H4 are deacetylated, and this hypoacetylated state is disrupted in mutants of *mis16*$^{+}$ and *mis18*$^{+}$ gene*s*, which are required for SpCENP-A loading (Hayashi et al., 2004). These results raised a possibility that Mcl1 and Swi7 might have a role at the

central domain in addition to outer centromeric heterochromatin.

Mcl1 is required for kinetochore function and structure. The central domain is associated with multiple protein complexes to form kinetochore that mediates the interaction between chromosome and spindle microtubules (Liu et al., 2005). I examined an involvement of Mcl1 in kinetochore function. First, TGS at this region was examined by introducing the *mcl1-101* mutation into an indicator strain, FY336 that harbors the *ura4*$^{+}$ gene inserted into the central domain (*cnt1*) (Allshire et al., 1995) (Fig. 9A). While the *wt* strain was resistant to 5-FOA, the *mcl1-101* mutant showed sensitivity to it, indicating that Mcl1 is required for TGS at the central domain. The *swi6Δ* mutant did not show alleviation of TGS at this region, consistent with a previous report (Partridge et al., 2000), which indicates that Swi6 does not associate with the central domain. In contrast, the *clr4Δ* mutant showed alleviation of TGS (see discussion). Finally, both of *swi7* mutants showed a defect in TGS at the central domain (Fig. 9B).

It was shown that the central domain forms a specialized chromatin structure distinct from outer centromere (Takahashi et al., 1992), and that integrity of TGS at the central domain correlates with that of the chromatin structure (Pidoux et al., 2003). To examine whether the specialized chromatin structure is disrupted in the *mcl1-101* mutant, micrococcal nuclease (MNase) assay was performed. Chromatin was prepared from log-phase cells grown at the restrictive temperature (36 ºC) for 6 hr, and partially digested by MNase, and DNA was subjected to Southern hybridization using probes corresponding to the central domain (*cnt1* and *imr1L*) and outer centromere (*otr1L*) of centromere I (Fig. 9C). In the *wt* strain, when hybridized with the *otr1L* probe, typical nucleosomal ladders were observed. The *cnt1* and *imr1L* probes showed smeared digestion patterns indicating

that these regions do not form regular nucleosome. In the *mcl1-101* mutant, however, these smeared digestion patterns were changed to ladder-like patterns at *imr1L* and, to lesser extent, at *cnt1*, indicating that the specialized chromatin structure is partially disrupted in the *mcl1-101* mutant. These results suggest that Mcl1 is required for maintaining the chromatin structure of kinetochore in addition to outer heterochromatin structure.

SpCENP-A loading onto kinetochore is diminished in the *mcl1* mutant. Although precise nature of the specialized chromatin structure at the central domain remains unknown, it was shown that only active, but not inactive, centromere forms this chromatin structure (Marschall and Clarke, 1995). More importantly, this structure was shown to be disrupted in mutants of SpCENP-A and also in mutants of its loading factors such as Mis6, Sim4 and Ams2 (Chen et al., 2003; Pidoux et al., 2003; Saitoh et al., 1997; Takahashi et al., 2000), indicating that SpCENP-A loading onto the central domain is essential for establishing or maintaining this structure. To examine the association of SpCENP-A to the central domain, N-terminally EYFP tagged SpCENP-A gene (*EYFP-cnp1*$^{+}$) was expressed in *mcl1-101* cells. In most *wt* cells, single spots of EYFP-SpCENP-A were observed (Fig. 10), and two or three spots were also observed in small portion of cells, which might undergo prometaphase or metaphase as reported previously (Takahashi et al., 2000). EYFP-SpCENP-A spots were observed in most *mcl1-101* cells (Fig. 10, cells indicated by arrowheads) similar to EGFP-SpCENP-A in the co-localization experiment (Fig 5). However, EYFP-SpCENP-A signal was weak or dispersed into the nucleus in many, but not all, separating *mcl1-101* cells (Fig. 10, cells indicated by asterisk). Since separating *S.pombe* cells undergo S-phase, above result

suggests that Mcl1 might be required for SpCENP-A association to the central domain during S-phase, and other pathways could load SpCENP-A in other phases of cell cycle.

Genetic interaction between Mcl1 and SpCENP-A. To further analyze the association of SpCENP-A to the central domain in the *mcl1-101* mutant, ChIP assay was attempted. The endogenous *cnp1*$^{+}$ gene was C-terminally tagged with 3x FLAG and 6x His (FH). Although Cnp1-FH was enriched at the central domain by ChIP assay (data not shown), the *cnp1-FH* strain showed a slightly slow growth and sensitivity to TBZ (Fig. 11A), indicating that *cnp1-FH* is a loss-of-function allele. I tried to introduce the *cnp1-FH* allele into various mutant backgrounds by genetic cross, and could obtain *cnp1-FH* strains in the *swi7-1*, *swi6Δ* and *hrp1Δ* (see below) backgrounds, but not in the *mcl1-101* background. This result was confirmed by tetrad analysis, showing that *cnp1-FH mcl1-101* strain was lethal (Fig. 11B and Table 3), suggesting that Mcl1 has a strong genetic interaction with SpCENP-A.

Overexpression of the *cnp1*$^{+}$ gene in SpCENP-A loading mutants, such as *mis6-302* and *ams2Δ*, results in partial suppression of temperature sensitivity or slow growth of these mutants (Chen et al., 2003; Hayashi et al., 2004). To examine whether phenotypes of the *mcl1-101* mutant are also suppressed by its overexpression, the multi-copy plasmid carrying the *cnp1*$^{+}$ gene was introduced, and temperature sensitivity and sensitivity to TBZ were observed. Neither temperature nor TBZ sensitivity was suppressed by overexpression of the *cnp1*$^{+}$ gene (Fig. 11C). Overexpression of the *cnp1*$^{+}$ gene suppressed the slow growth of the *ams2Δ* mutant, consistent with the previous report, and also partially recovered resistance to TBZ. These results suggest that increased level of SpCENP-A is not sufficient for suppressing defects in *mcl1-101* cells.

Mcl1 might belong to a novel SpCENP-A loading pathway distinct from Mis6 and Ams2 pathways. To understand a role of Mcl1 in SpCENP-A loading, I examined relationships of Mcl1 with two characterized SpCENP-A loading pathways, Mis6 and Ams2 pathways. Mis6 constitutively associates with the central domain depending on all other factors of Mis6 pathway (Hayashi et al., 2004; Pidoux et al., 2003), and is considered to be required for SpCENP-A loading during S phase and G2 phase (Takahashi et al., 2005). To examine whether Mcl1 is required for Mis6 association to the central domain, Mis6-GFP was expressed from the endogenous locus. Mis6-GFP formed one spot in the nucleus corresponding to the cluster of centromeres in most *wt* cells (Fig. 12A), consistent with previous reports (Saitoh et al., 1997). This localization was also observed in *mcl1-101* cells, including separating S phase cells (Fig. 12A). This result suggests that Mcl1 is dispensable for Mis6 loading onto the central domain.

Ams2 is a cell cycle regulated GATA factor and required for SpCENP-A loading possibly in S-phase (Chen et al., 2003). The *mcl1-101* mutant turned out to be synthetically lethal with the *ams2Δ* mutation (Fig. 12B and Table 3). Hrp1 is a member of CHD (chromo-ATPase/helicase-DNA binding domain) chromatin remodeling factors, and is required for SpCENP-A loading and histone hypoacetylation at the central domain (Walfridsson et al., 2005). In addition, Hrp1 was shown to belong to Ams2, but not to Mis6, pathway in SpCENP-A loading by examining genetic interactions between them (Walfridsson et al., 2005). The *mcl1-101 hrp1Δ* was viable, but dramatically reduced the permissive temperature for growth (Fig. 12C and Table 3). These genetic interactions suggest that Mcl1 might belong to an SpCENP-A loading pathway distinct from Ams2 and Hrp1.

Results

The *mcl1-101* mutant cell shows aberrant mitosis. Defect in sister chromatid cohesion results in premature separation of sister centromeres, which is frequently observed in cells harboring the *mcl1-1* mutation (Williams and McIntosh, 2002) that terminates at 124th codon of Mcl1 protein (815 amino acid), and the *mcl1-102* mutation (Tsutsui et al., 2005) that codes 1-268th amino acid and 11-unrelated C-terminal residues. Indeed, the *mcl1-1* mutant shows aberrant mitosis such as lagging chromosome, indicative of impaired sister chromatid cohesion, and unequal chromosome segregation (Williams and McIntosh, 2002). Another allele, the *mcl1-101* mutation causes temperature sensitivity for growth and has three point mutations at its C-terminal half, and results in Pro to Ser (493th), Leu to Phe (763th), and Ala to Val (768th) amino acid changes (Tsutsui et al., 2005). To examine mitotic phenotype of this mutant, *mcl1-101* cells were grown at 37 ºC for 6 hr before fixation and treatment with DAPI. Some portion of *mcl1-101* mutant cells showed unequal chromosome separation (Fig. 1A, arrows). The *mcl1Δ* mutant cell also showed unequal chromosome separation as well as lagging chromosomes (Fig. 1A), and the frequency of aberrant mitosis was higher than that in *mcl1-101* cells. This result indicates that *mcl1-101* mutant is defective in mitosis at the restrictive temperature, but it is relatively moderate compared to the null mutation. Although lagging chromosome was not detected in *mcl1-101* cells, the *mcl1-101* mutation was synthetic lethal with a conditional mutation of the *rad21*$^{+}$ gene, which encodes a non-SMC subunit of cohesin complex (Table 3), suggesting that *mcl1-101* cells also have a defect in sister chromatid cohesion, which produces lagging chromosomes. Since *mcl1Δ* and *mcl1-102* mutants cells show severe growth delay, the *mcl1-101* mutant

was used in the following experiments.

Genetic interaction between Mcl1 and DNA polymerase α, Swi7. In fission yeast, it was reported that loading of Swi6 onto heterochromatin requires DNA polymerase α catalytic subunit, Swi7 (Ahmed et al., 2001; Nakayama et al., 2001a). The *mcl1-101* mutant shows a slight reduction in its permissive growth temperature when combined with a mutation of the *swi7*$^{+}$ gene, *polα ts13* (Tsutsui et al., 2005), but this mutation does not show any defect in heterochromatin (Y. Tsutsui, unpublished result). To further analyze the relationship between Mcl1 and Swi7, I examined genetic interactions with other *swi7* alleles, *swi7-1* and *swi7-H4*, both of which were reported to be defective in the maintenance of heterochromatin (Fig. 1B). The *mcl1-101 swi7-H4* double mutant was viable, but showed an exceedingly reduced temperature for growth (Fig. 1C and Table 3) and showed an extremely elongated morphology at 30 ºC, which was similar to that of the *mcl1-101* single mutant cell at the restrictive temperature, 37 ºC (data not shown). The *swi7-1* mutation was synthetically lethal with the *mcl1-101* mutation even at 25 ºC (Fig. 1D and Table 3). These results suggest that Mcl1 and Swi7 have a functional link in chromatin regulation, and that Mcl1 might be also required for Swi6 loading as Swi7. Cohesin is known to be preferentially enriched at the outer centromere in Swi6-dependent manner (Bernard et al., 2001; Nonaka et al., 2002). As sister chromatid cohesion near centromere is compromised in *mcl1* mutants (Williams and McIntosh, 2002; Y. Tsutsui, unpublished result), I hypothesized that Mcl1 might be directly involved in the maintenance of heterochromatin in concert with Swi7 (that is, Swi6 loading), and contribute to sister chromatid cohesion at outer centromere indirectly.

Transcriptional gene silencing is alleviated in the *mcl1* mutant. To assess maintenance of heterochromatin in the *mcl1* mutant, we used three indicator strains as follows: FY1193 strain that harbors both *ura4*$^+$ gene (pyrimidine base biosynthesis) and *ade6*$^+$ gene (purine base metabolism) inserted into outer centromere (outer part of *imr* and *otr*) on centromere I (Allshire et al., 1995), FY597 strain that carries the *ura4*$^+$ gene inserted into centromere-distal side of *mat3M* loci (Allshire et al., 1995), and FY520 strain that harbors the *ura4*$^+$ gene adjacent to telomere on the non-essential mini-chromosome (Nimmo et al., 1994) (Fig. 2A-C). These marker genes inserted into heterochromatin are transcriptionally repressed, and this phenomenon is called transcriptional gene silencing (TGS). TGS can be used as an indicator of heterochromatin function since its alleviation is observed in mutants defective in heterochromatin assembly (Allshire et al., 1994; Allshire et al., 1995). TGS of these strains were assayed on EMM plates containing 5-FOA, which kills *ura4*$^+$-expressing cells, and on YE plates, which contains low concentration of adenine and changes colony color of *ade6*$^+$-expressing cells from red to white. The *mcl1-101* mutant harboring maker genes at outer centromere was more sensitive to 5-FOA and became pink on the low adenine plate compared to the wild-type (*wt*) strain (Fig. 2A). The level of alleviation in *mcl1-101* cells was comparable to that of *swi6Δ* cells at *imr* (FOA), but not at *otr* (Low adenine) in which *swi6Δ* cells showed more severe de-repression. In addition, *mcl1-101* cells also showed a defect in TGS at *mat* loci (Fig. 2B) and slightly at telomere (Fig. 2C). In agreement with previous reports, *swi7-H4* and *swi7-1* cells also showed alleviation of TGS at heterochromatic regions tested, except for telomere in *swi7-1* cells (Fig. 2A-C and data not shown). To confirm whether transcripts from heterochromatic regions are indeed increased, quantitative RT-PCR for the *ura4*$^+$ gene inserted into *imr* was

performed. While *swi6Δ* and *clr4Δ* mutants accumulated 5.8- and 18.1-fold *ura4*$^+$ transcripts compared to the *wt* strain, 2-fold increase in the transcripts was detected in the *mcl1-101* mutant at the semi-permissive temperature, 32 ºC (Fig. 2D). These results suggest that Mcl1 is involved in the maintenance of heterochromatin at three regions, possibly in concert with Swi7.

The role of Mcl1 in the maintenance of heterochromatin is unique among DNA replication apparatus. It is possible that alleviation of TGS observed in *mcl1-101* and *swi7* mutants might be an indirect consequence resulting from destabilized replication fork. To eliminate this possibility, TGS was examined in other replication-related mutants (Fig. 3A). The *polδ ts02* is a conditional mutation of a catalytic subunit of DNA polymerase δ, which is considered to have central roles in chromosomal DNA replication, DNA repair, and recombination (Hubscher et al., 2000). Both *rad2*$^+$ and *dna2*$^+$ genes code nucleases involved in Okazaki fragment processing. None of these mutants showed a defect in TGS at outer centromere (Fig. 3A). Furthermore, the null mutant of DNA replication-checkpoint gene, *rad3*$^+$, also did not show any alleviation of TGS at outer centromere (Fig. 3B). These results suggest that Mcl1 and Swi7 have a unique function among DNA replication machinery in the maintenance of heterochromatin.

Centromeric heterochromatin does not depend on integrity of sister chromatid cohesion. Next, TGS at outer centromere was examined in mutants deficient in sister chromatid cohesion. The *eso1*$^+$ gene was shown to be required for the establishment of sister chromatid cohesion during S-phase (Tanaka et al., 2000). The *ctf18*$^+$ gene is homologous to *S. cerevisiae CTF18*, which forms an alternative RFC

complex, and is also required for the establishment of sister chromatid cohesion (Mayer et al., 2001). The *ctf18Δ* mutant was viable, but showed increased mini-chromosome loss frequency (Y. Tsutsui, unpublished result). None of these mutants showed a defect in TGS at outer centromere (Fig. 3A). It was reported that a mutation of the *psc3*$^{+}$ gene, which encodes a non-SMC subunit of cohesin complex, shows no defect in TGS at outer centromere (Nonaka et al., 2002). These results support the idea that sister chromatid cohesion at outer centromere depends on centromeric heterochromatin, but not vise versa. Therefore Mcl1 might have a direct function in the maintenance of heterochromatin, which is essential for sister chromatid cohesion at outer centromere.

Endogenously repressed *mat2P* gene at *mat* loci is aberrantly expressed in the *mcl1-101* mutant. *S. pombe mat* loci are composed of expressed *mat1P/M* locus and silent *mat2P* and *mat3M* loci, and information of *mat1* locus (P or M) is switched by copy transposition (Beach, 1983). At least two pathways are known to redundantly repress the expression from the silent loci: *trans*-acting factors, such as Clr1-4 and Swi6, and *cis*-acting sequences near *mat2P* and *mat3M*. When combined with deletion of the *cis*-acting sequence near *mat2P* (*Bgl*II-*Bss*HII fragment), mutants of *clr1-4*, *swi6*, and *swi7* genes show severe de-repression of *mat2P* gene, resulting in the expression of both mating type genes which leads to aberrant meiosis in haploid cell, that is called “Haploid meiosis” (Ahmed et al., 2001; Nakayama et al., 2001a; Thon et al., 1994). To examine whether Mcl1 is required for repression of the silent loci, *mat2PΔ* (*Bgl*II-*Bss*HII) deletion was introduced into the *mcl1-101* mutant. Haploid meiosis can be easily detected by treating a colony with iodine vapor that stains resultant spores into brown. The *mcl1-101* mutant became light brown after treating with iodine vapor whereas the *wt* strain remained white

and the *swi6Δ* mutant turned dark brown (Fig. 4). This result indicates that Mcl1 is also required for repressing the expression of endogenously silenced *mat* loci.

Microscopic analysis of Swi6 localization to heterochromatic regions in the *mcl1* mutant. Swi6 is an essential component of heterochromatin and constitutively localizes to heterochromatic regions. This localization can be observed by immunostaining as two to four spots in the nucleus, which represent centromere, *mat* loci, and telomeres (Ekwall et al., 1995). In *clr4* mutant cells, Swi6 is delocalized from these regions, and dispersed within the nucleus (Ekwall et al., 1996). To observe Swi6 localization in the *mcl1-101* mutant, the *swi6*$^{+}$*-EYFP* gene was expressed under its own promoter. The *swi6*$^{+}$*-EYFP* strain was not sensitive to microtubule-destabilizing drug, TBZ, and did not show any defect in TGS at outer centromere, indicating that Swi6-EYFP is functional (Y. Akamatsu, personal communication). At the permissive temperature for *mcl1-101* (25 ºC), *wt* and *mcl1-101* cells formed one to four spots in the nucleus while *clr4Δ* cells did not, as reported previously (data not shown). Next, Swi6 localization was observed at the semi-permissive (32 ºC) and the restrictive temperature (37 ºC for 6 hr). As shown in Fig. 5A, in contrast to *wt* cells in which two major spots with some minor spots were observed, *mcl1-101* cells showed only one major spot with several faint spots at both temperatures. To examine which heterochromatic region retains Swi6 in *mcl1-101* cells, N-terminally EGFP tagged SpCENP-A gene (*EGFP-cnp1*$^{+}$) was expressed under *nmt41* promoter as a marker for centromere (Fig. 5B). In the most part of *mcl1-101* cells, EGFP-SpCENP-A localized at 37˚C when overexpressed. The major Swi6-spot remaining in *mcl1-101* cells at 37 ºC coincided with the EGFP-SpCENP-A signal, indicating that *mcl1-101* cells could retain Swi6 to centromere. Another spot that

became faint or disappeared in *mcl1-101* cells is discussed later.

In addition, the *chp1*$^{+}$ gene was endogenously tagged with GFP and its localization was observed in *mcl1-101* cells. Chp1 protein is a component of RITS complex required for targeting (that is, establishment) of heterochromatin to a specific site (Verdel et al., 2004), and also constitutively localizes to heterochromatic regions depending on the action of Clr4 (Sadaie et al., 2004). Chp1-GFP formed one to four spots in *mcl1-101* cells similar to *wt* cells (Fig. S1), indicating that Mcl1 is dispensable for RITS association to heterochromatic regions.

ChIP analysis of Swi6 localization to heterochromatic regions in the *mcl1* mutant. To further analyze localization of Swi6 in the *mcl1-101* mutant, chromatin immunoprecipitation (ChIP) assay was performed using same strains as in Fig. 5A. Precipitated DNA was quantified by real-time PCR using several sets of primers corresponding to heterochromatic regions and euchromatic regions (Fig. 6A). In the *wt* strain, Swi6-EYFP was enriched at heterochromatic regions such as outer centromere (*imr195*, *dg*, and *dh*), *mat* loci (*mat2P* and *cenH*), and telomere (*TEL*) compared to euchromatic regions (*ade6* and actin gene, *act1*) (Fig. 6B). In contrast, association of Swi6-EYFP at heterochromatic regions was abolished in the *clr4Δ* mutant, consistent with previous reports (Nakayama et al., 2001b). In the *mcl1-101* mutant, association of Swi6-EYFP to outer centromere (*imr195*, *dg*, and *dh*) was not impaired, or rather, slightly increased (1.5- to 1.8-fold). In addition, Swi6-EYFP association to the *ura4*$^{+}$ gene inserted into *imr* (Fig. 2A) was not decreased (Fig. S2). Swi6-EYFP enrichment at *mat* loci (*mat2P* and *cenH*) was slightly decreased (0.7-fold at both regions), while that of telomere (*TEL*) was comparable to the *wt* strain. Partial impairment of Swi6-EYFP

association was observed in the *swi7-H4* mutant: 0.59- to 0.65-fold at outer centromere, 0.43- to 0.45-fold at *mat* loci, and 0.71-fold at telomere). These results suggest that Mcl1 is dispensable for Swi6 localization to outer centromere and telomere in contrast to Swi7, but might have a subtle function at *mat* loci.

Mcl1 and Swi7 have a Swi6 independent function at centromere. To further assess the relationship between Mcl1 and Swi6, their genetic interaction was examined using microtubule-destabilizing drug, TBZ. Since mutants deficient in centromeric sister chromatid cohesion (that is, outer centromeric heterochromatin) or kinetochore function are known to be sensitive to TBZ, sensitivity to this drug can be used as an indicator of centromere integrity. The *mcl1-101 swi6Δ* double mutant was constructed and turned out to be viable with a slight slow growth. However, the double mutant showed a synergistic sensitivity to TBZ compared to each single mutant (Fig. 7A and Table 3). These results suggest that Mcl1 has Swi6-independent function in maintaining centromeric heterochromatin, or in other distinct processes. Interestingly, the *swi7-H4* mutant also showed a synergistic interaction with the *swi6Δ* mutation in TBZ sensitivity (Fig. 7A), indicating that Swi7 also might have a novel function at centromere other than Swi6 loading. In consistent with this idea, I found that both *mcl-101* and *swi7* mutants showed a higher sensitivity to TSA, which specifically inhibits HDAC activity (Yoshida et al., 1990) at the concentration of 25 μg/ml, at which neither the *wt* strain nor the *clr4Δ* mutant showed the sensitivity (Fig 7B). It was reported that transient treatment with TSA increased the level of histone acetylation at outer centromere and impaired centromeric heterochromatin (Ekwall et al., 1997). Thus Mcl1 and Swi7 might be implicated in outer centromeric heterochromatin by an HDAC-related process independent of Swi6-Clr4.

Furthermore, preferential centromeric localization of Rad21, a cohesin subunit, was not decreased in the *mcl1-101* mutant in contrast to the *swi6Δ* mutant (Fig. S3), suggesting that Mcl1 has an unknown role in centromeric cohesion distinct from cohesin localization.

Histone H4 at the outer heterochromatic domain and the central domain are hyper-acetylated in the *mcl1* mutant. As *mcl-101* and *swi7* mutants were found to be sensitive to TSA, I examined the acetylation state of histone H4 by ChIP assay using an antiserum against a peptide corresponding to amino acid 2-19 of histone H4 acetylated at K5, K8, K12 and K16. Acetylation at heterochromatic regions was increased by 2.3-fold (*imr-195*), 3.0-fold (*dg-223*), 2.2-fold (*cenH*) and 25-fold (*TEL*) in the *mcl1-101* mutant (Fig. 8B). Acetylation at euchromatic regions was also increased by 1.9-fold (*lys1*) and 1.4-fold (*ade6-2*), but degree of increase was relatively moderate compared to that of other regions. In the *swi7-1* mutant, however, no significant increase was observed in heterochromatic regions. The acetylation level of total histone H4 was not altered in the *mcl-101* mutant (Fig. 8C), indicating that increase in the acetylation is not a global phenomenon.

Unexpectedly, acetylation levels at the central domain were markedly increased in the *mcl1-101* mutant by 4-fold (*cnt-2*) and 5.3-fold (*imr-256*) compared to those in the *wt* strain (Fig. 8B). Increase of acetylation level was also observed in the *swi7-1* mutant at the central domain by 2.2-fold (*cnt-2*). At the central domain, N-terminal tails of histone H3 and H4 are deacetylated, and this hypoacetylated state is disrupted in mutants of *mis16*$^{+}$ and *mis18*$^{+}$ gene*s*, which are required for SpCENP-A loading (Hayashi et al., 2004). These results raised a possibility that Mcl1 and Swi7 might have a role at the

central domain in addition to outer centromeric heterochromatin.

Mcl1 is required for kinetochore function and structure. The central domain is associated with multiple protein complexes to form kinetochore that mediates the interaction between chromosome and spindle microtubules (Liu et al., 2005). I examined an involvement of Mcl1 in kinetochore function. First, TGS at this region was examined by introducing the *mcl1-101* mutation into an indicator strain, FY336 that harbors the *ura4*$^{+}$ gene inserted into the central domain (*cnt1*) (Allshire et al., 1995) (Fig. 9A). While the *wt* strain was resistant to 5-FOA, the *mcl1-101* mutant showed sensitivity to it, indicating that Mcl1 is required for TGS at the central domain. The *swi6Δ* mutant did not show alleviation of TGS at this region, consistent with a previous report (Partridge et al., 2000), which indicates that Swi6 does not associate with the central domain. In contrast, the *clr4Δ* mutant showed alleviation of TGS (see discussion). Finally, both of *swi7* mutants showed a defect in TGS at the central domain (Fig. 9B).

It was shown that the central domain forms a specialized chromatin structure distinct from outer centromere (Takahashi et al., 1992), and that integrity of TGS at the central domain correlates with that of the chromatin structure (Pidoux et al., 2003). To examine whether the specialized chromatin structure is disrupted in the *mcl1-101* mutant, micrococcal nuclease (MNase) assay was performed. Chromatin was prepared from log-phase cells grown at the restrictive temperature (36 ºC) for 6 hr, and partially digested by MNase, and DNA was subjected to Southern hybridization using probes corresponding to the central domain (*cnt1* and *imr1L*) and outer centromere (*otr1L*) of centromere I (Fig. 9C). In the *wt* strain, when hybridized with the *otr1L* probe, typical nucleosomal ladders were observed. The *cnt1* and *imr1L* probes showed smeared digestion patterns indicating

that these regions do not form regular nucleosome. In the *mcl1-101* mutant, however, these smeared digestion patterns were changed to ladder-like patterns at *imr1L* and, to lesser extent, at *cnt1*, indicating that the specialized chromatin structure is partially disrupted in the *mcl1-101* mutant. These results suggest that Mcl1 is required for maintaining the chromatin structure of kinetochore in addition to outer heterochromatin structure.

SpCENP-A loading onto kinetochore is diminished in the *mcl1* mutant. Although precise nature of the specialized chromatin structure at the central domain remains unknown, it was shown that only active, but not inactive, centromere forms this chromatin structure (Marschall and Clarke, 1995). More importantly, this structure was shown to be disrupted in mutants of SpCENP-A and also in mutants of its loading factors such as Mis6, Sim4 and Ams2 (Chen et al., 2003; Pidoux et al., 2003; Saitoh et al., 1997; Takahashi et al., 2000), indicating that SpCENP-A loading onto the central domain is essential for establishing or maintaining this structure. To examine the association of SpCENP-A to the central domain, N-terminally EYFP tagged SpCENP-A gene (*EYFP-cnp1*$^{+}$) was expressed in *mcl1-101* cells. In most *wt* cells, single spots of EYFP-SpCENP-A were observed (Fig. 10), and two or three spots were also observed in small portion of cells, which might undergo prometaphase or metaphase as reported previously (Takahashi et al., 2000). EYFP-SpCENP-A spots were observed in most *mcl1-101* cells (Fig. 10, cells indicated by arrowheads) similar to EGFP-SpCENP-A in the co-localization experiment (Fig 5). However, EYFP-SpCENP-A signal was weak or dispersed into the nucleus in many, but not all, separating *mcl1-101* cells (Fig. 10, cells indicated by asterisk). Since separating *S.pombe* cells undergo S-phase, above result

suggests that Mcl1 might be required for SpCENP-A association to the central domain during S-phase, and other pathways could load SpCENP-A in other phases of cell cycle.

Genetic interaction between Mcl1 and SpCENP-A. To further analyze the association of SpCENP-A to the central domain in the *mcl1-101* mutant, ChIP assay was attempted. The endogenous *cnp1*$^{+}$ gene was C-terminally tagged with 3x FLAG and 6x His (FH). Although Cnp1-FH was enriched at the central domain by ChIP assay (data not shown), the *cnp1-FH* strain showed a slightly slow growth and sensitivity to TBZ (Fig. 11A), indicating that *cnp1-FH* is a loss-of-function allele. I tried to introduce the *cnp1-FH* allele into various mutant backgrounds by genetic cross, and could obtain *cnp1-FH* strains in the *swi7-1*, *swi6Δ* and *hrp1Δ* (see below) backgrounds, but not in the *mcl1-101* background. This result was confirmed by tetrad analysis, showing that *cnp1-FH mcl1-101* strain was lethal (Fig. 11B and Table 3), suggesting that Mcl1 has a strong genetic interaction with SpCENP-A.

Overexpression of the *cnp1*$^{+}$ gene in SpCENP-A loading mutants, such as *mis6-302* and *ams2Δ*, results in partial suppression of temperature sensitivity or slow growth of these mutants (Chen et al., 2003; Hayashi et al., 2004). To examine whether phenotypes of the *mcl1-101* mutant are also suppressed by its overexpression, the multi-copy plasmid carrying the *cnp1*$^{+}$ gene was introduced, and temperature sensitivity and sensitivity to TBZ were observed. Neither temperature nor TBZ sensitivity was suppressed by overexpression of the *cnp1*$^{+}$ gene (Fig. 11C). Overexpression of the *cnp1*$^{+}$ gene suppressed the slow growth of the *ams2Δ* mutant, consistent with the previous report, and also partially recovered resistance to TBZ. These results suggest that increased level of SpCENP-A is not sufficient for suppressing defects in *mcl1-101* cells.

Mcl1 might belong to a novel SpCENP-A loading pathway distinct from Mis6 and Ams2 pathways. To understand a role of Mcl1 in SpCENP-A loading, I examined relationships of Mcl1 with two characterized SpCENP-A loading pathways, Mis6 and Ams2 pathways. Mis6 constitutively associates with the central domain depending on all other factors of Mis6 pathway (Hayashi et al., 2004; Pidoux et al., 2003), and is considered to be required for SpCENP-A loading during S phase and G2 phase (Takahashi et al., 2005). To examine whether Mcl1 is required for Mis6 association to the central domain, Mis6-GFP was expressed from the endogenous locus. Mis6-GFP formed one spot in the nucleus corresponding to the cluster of centromeres in most *wt* cells (Fig. 12A), consistent with previous reports (Saitoh et al., 1997). This localization was also observed in *mcl1-101* cells, including separating S phase cells (Fig. 12A). This result suggests that Mcl1 is dispensable for Mis6 loading onto the central domain.

Ams2 is a cell cycle regulated GATA factor and required for SpCENP-A loading possibly in S-phase (Chen et al., 2003). The *mcl1-101* mutant turned out to be synthetically lethal with the *ams2Δ* mutation (Fig. 12B and Table 3). Hrp1 is a member of CHD (chromo-ATPase/helicase-DNA binding domain) chromatin remodeling factors, and is required for SpCENP-A loading and histone hypoacetylation at the central domain (Walfridsson et al., 2005). In addition, Hrp1 was shown to belong to Ams2, but not to Mis6, pathway in SpCENP-A loading by examining genetic interactions between them (Walfridsson et al., 2005). The *mcl1-101 hrp1Δ* was viable, but dramatically reduced the permissive temperature for growth (Fig. 12C and Table 3). These genetic interactions suggest that Mcl1 might belong to an SpCENP-A loading pathway distinct from Ams2 and Hrp1.

Discussion

Genomic DNA is wrapped around the histone octamer to form nucleosome, and this basal unit is organized into a variety of higher-order chromatin structures depending on histone variants, histone modifications, and chromatin associated proteins. These chromatin structures are essential for many cellular processes, among which faithful chromosome segregation mediated by centromere is the most important event for cell viability. Although many proteins that constitute centromeric chromatin structures have been identified and analyzed, it has been not well understood how these structures are maintained during DNA replication. To address this important question, I have characterized fission yeast Mcl1 protein because it was thought that this protein might directly regulate outer centromeric heterochromatin structure. In agreement with this hypothesis, the *mcl1-101* mutant exhibited TGS defect at outer centromere as well as *mat* loci and telomere (Fig. 2). Although Mcl1 was not involved in Swi6 loading onto outer centromere and telomere in contract to Swi7 (Fig. 5 and 6B), further analysis suggested that not only Mcl1, but also Swi7 would have a Swi6 (and Clr4)-independent function(s) at centromere (Fig. 7 and Table 3). Interestingly, in the *mcl1-101* mutant, histone H4 was highly acetylated both in outer centromeric heterochromatin and in the central domain (Fig. 8B). Furthermore, TGS at the central domain was alleviated and the specialized chromatin structure at this region was disrupted in the *mcl1-101* mutant (Fig. 9). Based on these observations, I have concluded that DNA polymerase α accessory factor, Mcl1, is required for the maintenance of two distinct centromeric chromatin structures in concert with DNA polymerase α. Several lines of evidences, though not direct, support the idea that Mcl1 is present at replication fork (see below). This study has improved our

knowledge about the epigenetic inheritance of chromatin structures, kinetochore and centromeric heterochromatin, during DNA replication.

A role of Mcl1 in outer centromeric heterochromatin is independent or downstream of Swi6. In most of the mutants reported far, deficiency in heterochromatin function has been attributed to the delocalization of Swi6 in coincidence with the loss of K9 methylation of histone H3, which is catalyzed by Clr4 (Ekwall, 2004). Although methylation of histone H3-K9 is not examined, I suppose that the *mcl1-101* mutant would maintain H3-K9 methylation since Swi6 localization did not decrease in this mutant (Fig. 6B). The reason why Swi6 still localizes in the *mcl1-101* mutant where TGS is impaired could be explained by two following possibilities. First, Mcl1 might function downstream of Swi6-Clr4 proteins. It has been reported that *S. pombe* Hsk1 (Cdc7), a Dfp1 (Dbf4)-dependent protein kinase that regulates replication initiation, is required for preferential localization of cohesin to outer centromeric heterochromatin, which is mediated by dual interactions of Dfp1 with Swi6 and Psc3, a non-SMC subunit of cohesin complex (Bailis et al., 2003). Interestingly, *hsk1* and *dfp1* mutants show alleviation of TGS at outer centromere, but Swi6 normally localizes to outer centromere like the *mcl1-101* mutant while Psc3 does not (Bailis et al., 2003). These results indicate that the role of Hsk1-Dfp1 is downstream of Swi6 localization and upstream of cohesin localization at outer centromere. Recently, Hsk1-Dfp1 kinase activity has been shown to regulate Mcl1 association with S-phase chromatin and Swi7-containing complex (Williams and McIntosh, 2005), suggesting Mcl1 might belong to the same pathway as Hsk1-Dfp1. However, as enrichment of a cohesin subunit, Rad21, was observed at outer centromere in the *mcl1-101* mutant (Fig. S3B), this possibility seems not to be the case.

I favor another possibility that Mcl1 acts independent of Swi6/Clr4 pathway (Fig. 13, right). Since the *mcl1-101* mutant showed increase in acetylation level of histone H4 and sensitivity to TSA in contrast to *swi6Δ* and *clr4Δ* mutants (Fig. 8B and 7B), Mcl1 might recruit a certain HDAC(s) or modulate its activity. Similarly, *swi7* and *dfp1* mutants were sensitive to TSA (Fig. 7B and Fig. S4A), suggesting that Swi7 and Hsk1-Dfp1 are also involved in an HDAC-related process in addition to the Swi6-dependent process. These dual roles of Hsk1-Dfp1 and Swi7 can be interpreted as follows. Hsk1-Dfp1 stabilizes interaction between Mcl1 and Swi7 (Williams and McIntosh, 2005). In turn, Swi7 serves a platform for Mcl1 to recruit or regulate HDAC activity at the replication fork. In concert with this event, Swi7 recruits Swi6 to replicated daughter strands via its direct interaction (Nakayama et al., 2001a), and Hsk1-Dfp1 binds to Swi6 via Dfp1 and then passes cohesin complex to Swi6-deposited daughter strands (Bailis et al., 2003). In this model, malfunction of either Hsk-Dfp1 or Swi7 could lead to dissociation of Mcl1 from Swi7-containing replication complex and impairment of Mcl1-related HDAC function, which cause sensitivity to TSA (Fig. 7B and Fig. S4A). Although how Mcl1 recruits or regulates HDAC(s) activity is currently unclear, protein-protein interactions with HDAC(s) or HDAC-associated factor(s) through its N-terminus WD40 repeats domain might be important for regulating histone acetylation state.

Several HDACs are known to be required for outer centromeric heterochromatin and these include Clr3, Clr6, Sir2 and Hst4 (Freeman-Cook et al., 1999; Grewal et al., 1998; Nakayama et al., 2003; Shankaranarayana et al., 2003; Silverstein et al., 2003). Among them, Clr3 and Sir2 have been reported to be required for localization of Swi6 to outer centromere (Shankaranarayana et al., 2003; Yamada et al., 2005), suggesting that Mcl1-dependent histone acetylation does not depend on these HDACs. Clr6 forms a

stable SIN3 HDAC complex with a transcriptional co-repressor homologue Pst2 and some other factors, and this complex is required for maintaining hypoacetylated state of histone H3 and H4, and furthermore for sister chromatid cohesion at outer centromere (Nakayama et al., 2003; Silverstein et al., 2003). Although it is unclear whether Swi6 localization is retained or not, SIN3 complex-deficient cell is proficient for preferential localization of cohesin to outer centromere (Nakayama et al., 2003), suggesting that localization of cohesin itself is not sufficient for efficient sister chromatid cohesion. Interestingly, the *mcl1-101* mutant is also proficient for localization of the cohesin subunit Rad21 even at the restrictive temperature (Fig. S3B). Thus, I ague that Mcl1 might recruit or regulate Clr6 activity to outer centromere during DNA replication, and make a condition suitable for chromatin to be compact independent of Swi6, and for cohesin to form tight molecular glue (Fig. 13, right). A possibility that Mcl1 might regulate Hst4 activity could not be excluded at present.

Involvement of Mcl1 in the maintenance of heterochromatin at *mat* loci and telomere. In addition to outer centromere, Mcl1 is required for TGS at *mat* loci and telomere (Fig. 2B and C) and for repressing the endogenously silenced mating gene (Fig. 4). Microscopic analysis showed that one of major Swi6-EYFP spots were disappeared or diminished in *mcl1-101* cells at higher temperatures, and that this spot was not centromere signal (Fig. 5) By ChIP assay, Swi6-EYFP was shown to normally localize to telomere, but not to *mat* loci (Fig. 6B). Acetylated histone H4 accumulated at both *mat* loci and telomere in the *mcl1-101* mutant (Fig. 8B).

It has been suggested that heterochromatin at *mat* loci depends on two redundant mechanisms, RNAi- and Atf1/Pcr1-based machineries (Hall et al., 2002; Jia et

al., 2004; Kim et al., 2004). Atf1 and Pcr1 are stress-activated ATF/CREB family proteins that bind to *mat2/3* interval, and are required for recruiting Clr4 and Swi6 (Jia et al., 2004). Recent study has also suggested that Atf1/Pcr1 recruits Clr3, that acts on histone H3-K14 *in vivo* (Bjerling et al., 2002), to *mat2/3* interval to maintain histone modification patterns suitable for heterochromatin by inhibiting histone H3-K14 acetylation and H3-S10 phosphorylation, and by enhancing H3-K9 tri-methylation (Yamada et al., 2005). Although only histone H4 acetylation was examined in the *mcl1-101* mutant (Fig. 8B), Mcl1 might function along with Clr3 to maintain preferred histone modification pattern to recruit Swi6. Thus, at *mat* loci, Mcl1 might belong to Swi6 pathway in concert with Swi7, and the weakened Swi6-EYFP signal in *mcl1-101* cells might correspond to *mat* loci (Fig. 5). It is also plausible that the weakened signal might come from telomere defect although Swi6 association was comparable to *wt* strain in ChIP assay (Fig. 6B). This discrepancy can be interpreted as that telomeric clustering might be disrupted in *mcl1-101* cells as observed in RNAi-deficient cells (Hall et al., 2003). Increase in acetylation level at telomere might weaken unknown molecular glue that put together telomere ends.

Mcl1 is necessary for the specialized chromatin structure at the central domain. Accumulation of acetylated histone H4 at the central domain in *mcl1-101* and *swi7* mutants also raised a possibility that Mcl1/Swi7 might act on the central domain in addition to outer centromeric heterochromatin (Fig. 8B). Indeed, *mcl1-101* and *swi7* mutants, but not the *swi6Δ* mutant, showed alleviation of TGS at the central domain (Fig. 9A and 9B). As the central domain is not coated with Swi6 (Partridge et al., 2000) and thus TGS of this region might be caused by heterochromatin-independent mechanism, it

is possible that a variety of kinetochore proteins that associate to it or the specialized chromatin structure might inhibit access by transcription machinery. However, the *clr4Δ* mutant was also deficient in TGS at the central domain (Fig. 9A). Since histone H3 at the central domain is methylated at Lys-4, a hallmark of active chromatin, instead of Lys-9 (Cam et al., 2005), alleviation of TGS observed in the *clr4Δ* mutant might be indirect consequence. It is possible that loss of H3-K9 methylation and dissociation of all chromo-domain proteins that binds to it, such as Swi6, Chp1, and Chp2 (Sadaie et al., 2004), resulted in collapse of centromeric heterochromatin to lead to instability of the inner central domain. In this context, alleviation observed in *mcl1-101* and *swi7* mutants might also result from indirect effect of impaired outer heterochromatin as *clr4Δ*. Alleviation of TGS at outer heterochromatic domain was greater in *swi6Δ* than in *mcl1-101* and *swi7-H4* (Fig. 2A and 2D), suggesting that heterochromatin structure is more impaired in *swi6Δ*. However, only *mcl1-101* and *swi7-H4,* but not *swi6Δ,* showed a defect at the central domain (Fig. 9A), suggesting that alleviation of TGS at this region observed in *mcl1-101* and *swi7-H4* is not caused by indirect effect of impaired outer heterochromatin.

As shown in Fig. 9C, Mcl1 is necessary for the specialized chromatin structure, which is indicative of functional kinetochore (Marschall and Clarke, 1995). In consistent with this, *mcl1* cells showed unequal chromosome segregation (Fig. 1A), which reflects malfunction of kinetochore leading to mono-polar attachment of sister centromeres by one side of mitotic spindle. In the *mcl1-101* mutant, the smeared digestion pattern was greatly replaced with the ladder pattern at *imr1L*, but at *cnt1,* only slight alternation was detected (Fig. 9C). This is contrast to conditional *cnp1* and *mis6* mutants in which the smeared pattern at *cnt1* is completely replaced with the ladder pattern at 36 ºC (Saitoh et

al., 1997; Takahashi et al., 2000). Since *mcl1-101* cells could divide slowly in the condition for MNase assay (36 ºC) in which viability of *cnp1* and *mis6* cells dramatically decreased in 10 hr (Saitoh et al., 1997; Takahashi et al., 2000), residual activity of Mcl1 might be sufficient for maintaining the chromatin structure at innermost part of the central domain (*cnt1*). Alternatively, other overlapping pathways might maintain the structure at *cnt1*.

Mcl1 might belong to an SpCENP-A loading pathway distinct from Mis6 and Ams2. I have shown that *mcl1-101* mutation has a strong genetic interaction with the loss of function allele, *cnp1-FH* (Fig. 11B and Table 3), and that S-phase *mcl1-101* cells are deficient in SpCENP-A association to kinetochore (Fig. 10), suggesting that, like mutants of SpCENP-A and its loading factors, impaired SpCENP-A association might induce disruption of the specialized chromatin structure in *mcl1-101* cells (Fig, 9C). However, apparently normal EYFP-SpCENP-A signals were observed in most cells other than S-phase. This can be interpreted as that other loading pathways (G2-, M-, and G1-phase) could compensate for S-phase decrease in SpCENP-A association. This compensation is, however, not sufficient to recover the fully functional kinetochore since disruption of the specialized chromatin structure was observed in asynchronously growing *mcl1-101* cells (Fig. 9C). In *ams2Δ* cells, SpCENP-A dissociates from kinetochore only from S to mid-G2 phase, but they show severely impaired chromosome segregation (Chen et al., 2003).

At least two pathways are known to be responsible for SpCENP-A loading onto kinetochore (Takahashi et al., 2005). One is Mis6 pathway that is required for S- and G2-phase loading, and another is Ams2 pathway that functions in S-phase. Ams2 binds to the

central domain from G1/S to early G2 (Chen et al., 2003). Since Mcl1 physically interacts with DNA polymerase α and associates with S-phase chromatin (Tsutsui et al., 2005; Williams and McIntosh, 2005), I supposed that Mcl1 might function in Ams2 pathway. However, the *mcl1-101* mutation turned out to be synthetically lethal with *ams2Δ* mutation (Fig. 12B and Table 3), indicating that Mcl1 acts on SpCENP-A loading in parallel with Ams2. On the other hand, Mis6 could normally localize to the central domain in *mcl1-101* cells (Fig. 12A), suggesting that Mcl1 is not required for Mis6 loading. It is possible that synthetic lethality of *mcl1-101 ams2Δ* might result from synthetic effect of impaired kinetochore (*ams2Δ* and *mcl1-101*) and outer heterochromatic domain (*mcl1-101*), leaving a possibility that Mcl1 might belong to Ams2 pathway. Furthermore, it also remains possible that Mcl1 might belong to Mis6 pathway by acting downstream of Mis6 localization. However I suggest that Mcl1 belongs to the third pathway as follows (Fig. 13, left). Acetylation level of histone H4 was elevated at the central domain in *mcl1-101* cells (Fig. 8B). Furthermore, drastic increase in acetylation level at *imr256* correlated with the extent loss of the specialized chromatin structure at *imr1L* (Fig. 8B and 9C), indicating that Mcl1 maintains kinetochore structure by regulating histone deacetylation. Mis16 shows a similarity to human retinoblastoma-associated protein, RbAp46 and RbAp48, which form two distinct histone deacetylase (HDAC) complexes, (Tong et al., 1998; Xue et al., 1998; Zhang et al., 1997; Zhang et al., 1998). Mis16 is required for Mis6 localization, which leads to SpCENP-A association to kinetochore, and is also necessary for hypoacetylated state of histone H3 and H4 (Hayashi et al., 2004). In addition, Mis16 and its interacting partner, Mis18, are considered to be the most upstream components of Mis6 pathway. However, importance of Mis16/18-dependent histone deacetylation in Mis6 loading remains to be

unclear. Thus there is a possibility that Mis16/18 might be directly involved in SpCENP-A loading by regulating HDAC activity independent of Mis6 as suggested by Hayashi et al. (Hayashi et al., 2004). Therefore I propose that Mcl1 and Swi7 might mediate histone deacetylation during DNA replication by controlling unknown Mis16/18-containing HDAC complex (Fig. 13, left). Since the *dfp1* mutant did not show any defect in TGS at the central domain (Fig. S4B), Hsk1-Dfp1 complex might not be involved in this process.

It is exactly unknown that which HDAC(s) maintains hypoacetylated state of histone H3 and H4 at the central domain. However, several previous reports have given a clue to this question. First, alleviation of TGS at the central domain is reported in mutants of Clr3 and Hst4 (Freeman-Cook et al., 1999; Grewal et al., 1998). Secondly, by ChIP assay, Sir2 is shown to be enriched at the central domain although the *sir2Δ* mutant does not show any defect in TGS at this region (Freeman-Cook et al., 2005). Whether Clr3 and Hst4 associate with the central domain is unknown. Interestingly, *mcl1-101 sir2Δ* cells, but not *mcl1-101 hst4Δ* cells, showed synergistic sensitivity to TSA compared to each single mutant (Fig. S5 and Table 3). In addition, slow growth of *hst4Δ* cells was suppressed by *mcl1-101* mutation (Fig. S5 and Table 3). Although there are many possibilities, these genetic interactions could be interpreted as that Mcl1 regulates or recruits Hst4 activity to maintain hypoacetylated state of the central domain. Further experiments should unveil the HDAC(s) that acts on the central domain.

Mcl1 is a novel type of factor that is required for both kinetochore and outer centromeric heterochromatin structures. Most centromere proteins reported so far are necessary for one of kinetochore or outer heterochromatin structure (Pidoux and Allshire, 2004). For instance, the mutation of *mis6*$^{+}$ alleviates TGS only at the central

domain while the mutation of *swi6*$^{+}$ does only at the outer heterochromatin (Fig. 2A, 9A and Pidoux et al., 2003). In this study, I have shown that Mcl1 is a novel type of factor that maintains both structures of the complex centromere in fission yeast. Since Mcl1 disperses in the nucleus rather than makes foci throughout cell cycle, and it binds to chromatin only in S-phase (Williams and McIntosh, 2005), I suppose that Mcl1 associates with the replication fork via Swi7, and transiently localizes to centromere in early S-phase, when centromere is replicated (Kim et al., 2003). Recently, this new type of factor has been reported by Walfridsson et al. (Walfridsson et al., 2005). The CHD chromatin remodeling factor, Hrp1 is necessary for TGS at the central domain as well as outer centromere and *mat* loci, and localizes to centromere only in early S-phase (timing of HU arrest). Like *mcl1-101* cells, *hrp1Δ* cells show impaired SpCENP-A association and elevated histone acetylation at the central domain. Although genetic interaction experiments have shown that Mcl1 and Hrp1 might belong to distinct pathways (Fig. 12C), I could not preclude a possibility that Mcl1 might enhance histone deacetylation via chromatin remodeling as reported in human NuRD complex (Tong et al., 1998; Xue et al., 1998; Zhang et al., 1998).

Mcl1 is well conserved from yeast to human, but counterparts in higher eukaryotes remain to be examined. Interestingly, *S. cerevisiae* Ctf4 is also important for transcriptional gene silencing at *HMR* and telomere (Suter et al., 2004). Since HP1/Swi6 and histone H3-K9 methylation appear not to be conserved in *S. cerevisiae*, Swi6-idependent role of Mcl1 is reasonable. From these facts, I suppose that Mcl1 family are involved in more fundamental processes in chromatin regulation. This protein family contain WD40 repeats domain in N-terminus that forms β-propeller structure, providing a platform for protein-protein interaction (Smith et al., 1999). Since proteins that interact

with this domain of Mcl1 are unknown, identification of associating partners of Mcl1 is essential to further understand how chromatin structures are maintained during DNA replication.

Histone deacetylation and replication fork passage. As discussed above, Mcl1 is thought to be important for histone deacetylation though some HDACs both at kinetochore and at heterochromatin regions**.** Why is histone deacetylation during DNA replication important for maintaining these chromatin structures? It is known that newly synthesized histone H3 and H4 exhibit specific acetylation patterns shortly after they are incorporated into chromatin (Sobel et al., 1995) and when they are associating with chromatin assembly factor (CAF-1) (Verreault et al., 1996). Thus, one reasonable explanation is that the deposition-related acetylation of histone H3 and H4 must be immediately removed to reassemble appropriate chromatin structures after replication fork has passed. Another plausible explanation could be given by analogy to transcription. Histone acetylation is known to be important for transcriptional activation since several histone acetyltransferase (HATs) participate in this process (Grunstein, 1997). For example, the SAGA (Spt-Ada-Gcn5-Acetyltransferase) is a Gcn5-dependent HAT complex and activates transcription by acetylating N-terminal tail of histone H3 and H2B (Grant et al., 1997). In addition, the FACT (facilitates chromatin transcription) complex is required for RNA polymerase II-driven transcript elongation through nucleosome by removing histone H2A-H2B dimer (Belotserkovskaya et al., 2003), and Spt16 subunit of the *S. cerevisiae* FACT complex interacts with Sas3 HAT, coupling transcript elongation with histone acetylation (John et al., 2000). On the other hand, it has been recently shown that cotranscriptional histone H3-K36 methylation by PolII-associated Set2 recruits

Rpd3S HDAC complex, leading to deacetylation of transcripted regions, which is required to restore chromatin to its original state (Carrozza et al., 2005; Keogh et al., 2005). Since DNA replication machinery also must overcome repressive nature of chromatin, transient acetylation and subsequent deacetylation of replicated regions might be important to inherit chromatin structures to sister chromosomes. Interestingly *S. cerevisiae* FACT complex is also implicated in replication (Schlesinger and Formosa, 2000), and the *S. cerevisiae* Mcl1 homologue Ctf4 and Spt16 associate with DNA polymerase α in temporal-ordered manner during S-phase (Zhou and Wang, 2004), suggesting Mcl1 might be required to erase chromatin state suitable for replication fork passage produced by FACT complex. Although further studies is necessary to improve these expectations, results observed here would provide a novel insight into the close link between DNA replication apparatus and histone acetylation state in the epigenetic inheritance of chromatin structures.

Acknowledgment

I am grateful to Dr. Yasuhiro Tsutsui and Prof. Fumiaki Yamao of National Institute of Genetics (NIG) for guiding me to studies and helpful discussion during the doctor course. I am also grateful to Ms. Emi Fukuchi and Ms. Terumi Nishimura of our laboratory for supporting my experiments. I thank to Dr. Hiroaki Seino and Dr. Takahiro Nakayama in NIG for providing materials and for helpful discussion. I am thankful to Mr. Shunsuke Kimura and Dr. Tamotsu Yoshimori in NIG for supporting microscopic observations in this study. I also thank to Dr. Hiroshi Iwasaki of Yokohama City University for encouraging me in my project. *S. pombe* strains used in this study were kindly provided by Dr. Takashi Morishita, Dr. Hiroshi Mitsuzawa, Dr. Hiroto Okayama, Dr. Osami Niwa, Dr. Teresa S.-F. Wang, Dr. Grant W. Brown, Dr. Robin C. Allshire, and Dr. Shiv. I. S. Grewal. I am also thankful to Dr. Hiroyuki Araki, Dr. Hironori Niki, Dr. Tetsuji Kakutani, and Dr. Yasushi Hiromi of Progress Report Committee in NIG for giving advices on my project. I also thank to the members of NIG soccer team, “Prisoners” for sharing my joys and sorrows in Mishima life with me. Finally I thanks to my parents for supporting my life until today.

References

Ahmed, S., Saini, S., Arora, S., and Singh, J. (2001). Chromodomain protein Swi6-mediated role of DNA polymerase alpha in establishment of silencing in fission Yeast. J Biol Chem *276*, 47814-47821.

Allshire, R. C., Javerzat, J. P., Redhead, N. J., and Cranston, G. (1994). Position effect variegation at fission yeast centromeres. Cell *76*, 157-169.

Allshire, R. C., Nimmo, E. R., Ekwall, K., Javerzat, J. P., and Cranston, G. (1995). Mutations derepressing silent centromeric domains in fission yeast disrupt chromosome segregation. Genes Dev *9*, 218-233.

Bahler, J., Wu, J. Q., Longtine, M. S., Shah, N. G., McKenzie, A., 3rd, Steever, A. B., Wach, A., Philippsen, P., and Pringle, J. R. (1998). Heterologous modules for efficient and versatile PCR-based gene targeting in *Schizosaccharomyces pombe*. Yeast *14*, 943-951.

Bailis, J. M., Bernard, P., Antonelli, R., Allshire, R. C., and Forsburg, S. L. (2003). Hsk1-Dfp1 is required for heterochromatin-mediated cohesion at centromeres. Nat Cell Biol *5*, 1111-1116.

Basi, G., Schmid, E., and Maundrell, K. (1993). TATA box mutations in the *Schizosaccharomyces pombe nmt1* promoter affect transcription efficiency but not the transcription start point or thiamine repressibility. Gene *123*, 131-136.

Beach, D. (1983). Cell type switching by DNA transposition in fission yeast. Nature *305*, 682-688.

Belotserkovskaya, R., Oh, S., Bondarenko, V. A., Orphanides, G., Studitsky, V. M., and Reinberg, D. (2003). FACT facilitates transcription-dependent nucleosome

alteration. Science *301*, 1090-1093.

Bernard, P., Maure, J. F., Partridge, J. F., Genier, S., Javerzat, J. P., and Allshire, R. C. (2001). Requirement of heterochromatin for cohesion at centromeres. Science *294*, 2539-2542.

Bjerling, P., Silverstein, R. A., Thon, G., Caudy, A., Grewal, S., and Ekwall, K. (2002). Functional divergence between histone deacetylases in fission yeast by distinct cellular localization and in vivo specificity. Mol Cell Biol *22*, 2170-2181.

Boyes, J., Omichinski, J., Clark, D., Pikaart, M., and Felsenfeld, G. (1998). Perturbation of nucleosome structure by the erythroid transcription factor GATA-1. J Mol Biol *279*, 529-544.

Cam, H. P., Sugiyama, T., Chen, E. S., Chen, X., FitzGerald, P. C., and Grewal, S. I. (2005). Comprehensive analysis of heterochromatin- and RNAi-mediated epigenetic control of the fission yeast genome. Nat Genet *37*, 809-819.

Carrozza, M. J., Li, B., Florens, L., Suganuma, T., Swanson, S. K., Lee, K. K., Shia, W. J., Anderson, S., Yates, J., Washburn, M. P., and Workman, J. L. (2005). Histone H3 methylation by Set2 directs deacetylation of coding regions by Rpd3S to suppress spurious intragenic transcription. Cell *123*, 581-592.

Chen, E. S., Saitoh, S., Yanagida, M., and Takahashi, K. (2003). A cell cycle-regulated GATA factor promotes centromeric localization of CENP-A in fission yeast. Mol Cell *11*, 175-187.

Chikashige, Y., Kinoshita, N., Nakaseko, Y., Matsumoto, T., Murakami, S., Niwa, O., and Yanagida, M. (1989). Composite motifs and repeat symmetry in *S. pombe* centromeres: direct analysis by integration of NotI restriction sites. Cell *57*, 739-751.

Cirillo, L. A., Lin, F. R., Cuesta, I., Friedman, D., Jarnik, M., and Zaret, K. S. (2002). Opening of compacted chromatin by early developmental transcription factors HNF3 (FoxA) and GATA-4. Mol Cell *9*, 279-289.

Clarke, L., and Baum, M. P. (1990). Functional analysis of a centromere from fission yeast: a role for centromere-specific repeated DNA sequences. Mol Cell Biol *10*, 1863-1872.

Cottarel, G., Shero, J. H., Hieter, P., and Hegemann, J. H. (1989). A 125-base-pair CEN6 DNA fragment is sufficient for complete meiotic and mitotic centromere functions in *Saccharomyces cerevisiae*. Mol Cell Biol *9*, 3342-3349.

Ekwall, K. (2004). The roles of histone modifications and small RNA in centromere function. Chromosome Res *12*, 535-542.

Ekwall, K., Javerzat, J. P., Lorentz, A., Schmidt, H., Cranston, G., and Allshire, R. (1995). The chromodomain protein Swi6: a key component at fission yeast centromeres. Science *269*, 1429-1431.

Ekwall, K., Nimmo, E. R., Javerzat, J. P., Borgstrom, B., Egel, R., Cranston, G., and Allshire, R. (1996). Mutations in the fission yeast silencing factors *clr4*$^+$ and *rik1*$^+$ disrupt the localisation of the chromo domain protein Swi6p and impair centromere function. J Cell Sci *109 (Pt 11)*, 2637-2648.

Ekwall, K., Olsson, T., Turner, B. M., Cranston, G., and Allshire, R. C. (1997). Transient inhibition of histone deacetylation alters the structural and functional imprint at fission yeast centromeres. Cell *91*, 1021-1032.

Ekwall, K., and Partridge., J. F. (1999). Fission yeast chromosomal analysis: fluorescent in situ hybridisation (FISH) and chromatin immunoprecipitation (CHIP). W A Bickmore (ed), Chromsome structural analysis: a practical approach Oxford

University Press, Oxford, United Kingdom, 39-57.

Freeman-Cook, L. L., Gomez, E. B., Spedale, E. J., Marlett, J., Forsburg, S. L., Pillus, L., and Laurenson, P. (2005). Conserved locus-specific silencing functions of *Schizosaccharomyces pombe sir2*$^{+}$. Genetics *169*, 1243-1260.

Freeman-Cook, L. L., Sherman, J. M., Brachmann, C. B., Allshire, R. C., Boeke, J. D., and Pillus, L. (1999). The *Schizosaccharomyces pombe hst4*$^{+}$ gene is a *SIR2* homologue with silencing and centromeric functions. Mol Biol Cell *10*, 3171-3186.

Grant, P. A., Duggan, L., Cote, J., Roberts, S. M., Brownell, J. E., Candau, R., Ohba, R., Owen-Hughes, T., Allis, C. D., Winston, F.*, et al.* (1997). Yeast Gcn5 functions in two multisubunit complexes to acetylate nucleosomal histones: characterization of an Ada complex and the SAGA (Spt/Ada) complex. Genes Dev *11*, 1640-1650.

Grewal, S. I., Bonaduce, M. J., and Klar, A. J. (1998). Histone deacetylase homologs regulate epigenetic inheritance of transcriptional silencing and chromosome segregation in fission yeast. Genetics *150*, 563-576.

Grunstein, M. (1997). Histone acetylation in chromatin structure and transcription. Nature *389*, 349-352.

Hahnenberger, K. M., Carbon, J., and Clarke, L. (1991). Identification of DNA regions required for mitotic and meiotic functions within the centromere of *Schizosaccharomyces pombe* chromosome I. Mol Cell Biol *11*, 2206-2215.

Hall, I. M., Noma, K., and Grewal, S. I. (2003). RNA interference machinery regulates chromosome dynamics during mitosis and meiosis in fission yeast. Proc Natl Acad Sci U S A *100*, 193-198.

Hall, I. M., Shankaranarayana, G. D., Noma, K., Ayoub, N., Cohen, A., and Grewal, S. I.

(2002). Establishment and maintenance of a heterochromatin domain. Science *297*, 2232-2237.

Hanna, J. S., Kroll, E. S., Lundblad, V., and Spencer, F. A. (2001). *Saccharomyces cerevisiae CTF18* and *CTF4* are required for sister chromatid cohesion. Mol Cell Biol *21*, 3144-3158.

Hayashi, T., Fujita, Y., Iwasaki, O., Adachi, Y., Takahashi, K., and Yanagida, M. (2004). Mis16 and Mis18 are required for CENP-A loading and histone deacetylation at centromeres. Cell *118*, 715-729.

Hubscher, U., Nasheuer, H. P., and Syvaoja, J. E. (2000). Eukaryotic DNA polymerases, a growing family. Trends Biochem Sci *25*, 143-147.

Jia, S., Noma, K., and Grewal, S. I. (2004). RNAi-independent heterochromatin nucleation by the stress-activated ATF/CREB family proteins. Science *304*, 1971-1976.

John, S., Howe, L., Tafrov, S. T., Grant, P. A., Sternglanz, R., and Workman, J. L. (2000). The something about silencing protein, Sas3, is the catalytic subunit of NuA3, a yTAF(II)30-containing HAT complex that interacts with the Spt16 subunit of the yeast CP (Cdc68/Pob3)-FACT complex. Genes Dev *14*, 1196-1208.

Kaiser, C., Michaelis, S., and Mitchel, A. (1994). Methods in yeast genetics, 1994 edition. Cold Spring Harbor Laboratory Press, Cold Spring Harbor, N.Y.

Kang, H. Y., Choi, E., Bae, S. H., Lee, K. H., Gim, B. S., Kim, H. D., Park, C., MacNeill, S. A., and Seo, Y. S. (2000). Genetic analyses of *Schizosaccharomyces pombe dna2*$^{+}$ reveal that dna2 plays an essential role in Okazaki fragment metabolism. Genetics *155*, 1055-1067.

Keogh, M. C., Kurdistani, S. K., Morris, S. A., Ahn, S. H., Podolny, V., Collins, S. R.,

Schuldiner, M., Chin, K., Punna, T., Thompson, N. J., *et al.* (2005). Cotranscriptional set2 methylation of histone H3 lysine 36 recruits a repressive Rpd3 complex. Cell *123*, 593-605.

Kim, H. S., Choi, E. S., Shin, J. A., Jang, Y. K., and Park, S. D. (2004). Regulation of Swi6/HP1-dependent heterochromatin assembly by cooperation of components of the mitogen-activated protein kinase pathway and a histone deacetylase Clr6. J Biol Chem *279*, 42850-42859.

Kim, S. M., Dubey, D. D., and Huberman, J. A. (2003). Early-replicating heterochromatin. Genes Dev *17*, 330-335.

Kouprina, N., Tsouladze, A., Koryabin, M., Hieter, P., Spencer, F., and Larionov, V. (1993). Identification and genetic mapping of CHL genes controlling mitotic chromosome transmission in yeast. Yeast *9*, 11-19.

Liu, X., McLeod, I., Anderson, S., Yates, J. R., 3rd, and He, X. (2005). Molecular analysis of kinetochore architecture in fission yeast. EMBO J *24*, 2919-2930.

Lorentz, A., Ostermann, K., Fleck, O., and Schmidt, H. (1994). Switching gene swi6, involved in repression of silent mating-type loci in fission yeast, encodes a homologue of chromatin-associated proteins from Drosophila and mammals. Gene *143*, 139-143.

Marschall, L. G., and Clarke, L. (1995). A novel cis-acting centromeric DNA element affects *S. pombe* centromeric chromatin structure at a distance. J Cell Biol *128*, 445-454.

Mayer, M. L., Gygi, S. P., Aebersold, R., and Hieter, P. (2001). Identification of RFC(Ctf18p, Ctf8p, Dcc1p): an alternative RFC complex required for sister chromatid cohesion in *S. cerevisiae*. Mol Cell *7*, 959-970.

Measday, V., Hailey, D. W., Pot, I., Givan, S. A., Hyland, K. M., Cagney, G., Fields, S., Davis, T. N., and Hieter, P. (2002). Ctf3p, the Mis6 budding yeast homolog, interacts with Mcm22p and Mcm16p at the yeast outer kinetochore. Genes Dev *16*, 101-113.

Miles, J., and Formosa, T. (1992). Evidence that POB1, a *Saccharomyces cerevisiae* protein that binds to DNA polymerase alpha, acts in DNA metabolism in vivo. Mol Cell Biol *12*, 5724-5735.

Moreno, S., Klar, A., and Nurse, P. (1991). Molecular genetic analysis of fission yeast *Schizosaccharomyces pombe*. Methods Enzymol *194*, 795-823.

Nakayama, J., Allshire, R. C., Klar, A. J., and Grewal, S. I. (2001a). A role for DNA polymerase alpha in epigenetic control of transcriptional silencing in fission yeast. EMBO J *20*, 2857-2866.

Nakayama, J., Rice, J. C., Strahl, B. D., Allis, C. D., and Grewal, S. I. (2001b). Role of histone H3 lysine 9 methylation in epigenetic control of heterochromatin assembly. Science *292*, 110-113.

Nakayama, J., Xiao, G., Noma, K., Malikzay, A., Bjerling, P., Ekwall, K., Kobayashi, R., and Grewal, S. I. (2003). Alp13, an MRG family protein, is a component of fission yeast Clr6 histone deacetylase required for genomic integrity. EMBO J *22*, 2776-2787.

Nimmo, E. R., Cranston, G., and Allshire, R. C. (1994). Telomere-associated chromosome breakage in fission yeast results in variegated expression of adjacent genes. EMBO J *13*, 3801-3811.

Nishihashi, A., Haraguchi, T., Hiraoka, Y., Ikemura, T., Regnier, V., Dodson, H., Earnshaw, W. C., and Fukagawa, T. (2002). CENP-I is essential for centromere

function in vertebrate cells. Dev Cell *2*, 463-476.

Niwa, O., Matsumoto, T., Chikashige, Y., and Yanagida, M. (1989). Characterization of *Schizosaccharomyces pombe* minichromosome deletion derivatives and a functional allocation of their centromere. EMBO J *8*, 3045-3052.

Nonaka, N., Kitajima, T., Yokobayashi, S., Xiao, G., Yamamoto, M., Grewal, S. I., and Watanabe, Y. (2002). Recruitment of cohesin to heterochromatic regions by Swi6/HP1 in fission yeast. Nat Cell Biol *4*, 89-93.

Okuno, Y., Okazaki, T., and Masukata, H. (1997). Identification of a predominant replication origin in fission yeast. Nucleic Acids Res *25*, 530-537.

Partridge, J. F., Borgstrom, B., and Allshire, R. C. (2000). Distinct protein interaction domains and protein spreading in a complex centromere. Genes Dev *14*, 783-791.

Pidoux, A., Mellone, B., and Allshire, R. (2004). Analysis of chromatin in fission yeast. Methods *33*, 252-259.

Pidoux, A. L., and Allshire, R. C. (2004). Kinetochore and heterochromatin domains of the fission yeast centromere. Chromosome Res *12*, 521-534.

Pidoux, A. L., Richardson, W., and Allshire, R. C. (2003). Sim4: a novel fission yeast kinetochore protein required for centromeric silencing and chromosome segregation. J Cell Biol *161*, 295-307.

Polizzi, C., and Clarke, L. (1991). The chromatin structure of centromeres from fission yeast: differentiation of the central core that correlates with function. J Cell Biol *112*, 191-201.

Sadaie, M., Iida, T., Urano, T., and Nakayama, J. (2004). A chromodomain protein, Chp1, is required for the establishment of heterochromatin in fission yeast. EMBO J *23*, 3825-3835.

Saitoh, S., Takahashi, K., and Yanagida, M. (1997). Mis6, a fission yeast inner centromere protein, acts during G1/S and forms specialized chromatin required for equal segregation. Cell *90*, 131-143.

Schlesinger, M. B., and Formosa, T. (2000). POB3 is required for both transcription and replication in the yeast *Saccharomyces cerevisiae*. Genetics *155*, 1593-1606.

Schueler, M. G., Higgins, A. W., Rudd, M. K., Gustashaw, K., and Willard, H. F. (2001). Genomic and genetic definition of a functional human centromere. Science *294*, 109-115.

Shankaranarayana, G. D., Motamedi, M. R., Moazed, D., and Grewal, S. I. (2003). Sir2 regulates histone H3 lysine 9 methylation and heterochromatin assembly in fission yeast. Curr Biol *13*, 1240-1246.

Silverstein, R. A., Richardson, W., Levin, H., Allshire, R., and Ekwall, K. (2003). A new role for the transcriptional corepressor SIN3; regulation of centromeres. Curr Biol *13*, 68-72.

Smith, T. F., Gaitatzes, C., Saxena, K., and Neer, E. J. (1999). The WD repeat: a common architecture for diverse functions. Trends Biochem Sci *24*, 181-185.

Sobel, R. E., Cook, R. G., Perry, C. A., Annunziato, A. T., and Allis, C. D. (1995). Conservation of deposition-related acetylation sites in newly synthesized histones H3 and H4. Proc Natl Acad Sci U S A *92*, 1237-1241.

Sugiyama, T., Cam, H., Verdel, A., Moazed, D., and Grewal, S. I. (2005). RNA-dependent RNA polymerase is an essential component of a self-enforcing loop coupling heterochromatin assembly to siRNA production. Proc Natl Acad Sci U S A *102*, 152-157.

Takahashi, K., Chen, E. S., and Yanagida, M. (2000). Requirement of Mis6 centromere

connector for localizing a CENP-A-like protein in fission yeast. Science *288*, 2215-2219.

Takahashi, K., Murakami, S., Chikashige, Y., Funabiki, H., Niwa, O., and Yanagida, M. (1992). A low copy number central sequence with strict symmetry and unusual chromatin structure in fission yeast centromere. Mol Biol Cell *3*, 819-835.

Takahashi, K., Takayama, Y., Masuda, F., Kobayashi, Y., and Saitoh, S. (2005). Two distinct pathways responsible for the loading of CENP-A to centromeres in the fission yeast cell cycle. Philos Trans R Soc Lond B Biol Sci *360*, 595-606; discussion 606-597.

Takahashi, K., Yamada, H., and Yanagida, M. (1994). Fission yeast minichromosome loss mutants mis cause lethal aneuploidy and replication abnormality. Mol Biol Cell *5*, 1145-1158.

Tanaka, K., Yonekawa, T., Kawasaki, Y., Kai, M., Furuya, K., Iwasaki, M., Murakami, H., Yanagida, M., and Okayama, H. (2000). Fission yeast Eso1p is required for establishing sister chromatid cohesion during S phase. Mol Cell Biol *20*, 3459-3469.

Thon, G., Cohen, A., and Klar, A. J. (1994). Three additional linkage groups that repress transcription and meiotic recombination in the mating-type region of *Schizosaccharomyces pombe*. Genetics *138*, 29-38.

Tong, J. K., Hassig, C. A., Schnitzler, G. R., Kingston, R. E., and Schreiber, S. L. (1998). Chromatin deacetylation by an ATP-dependent nucleosome remodelling complex. Nature *395*, 917-921.

Tsutsui, Y., Morishita, T., Natsume, T., Yamashita, K., Iwasaki, H., Yamao, F., and Shinagawa, H. (2005). Genetic and physical interactions between

Schizosaccharomyces pombe Mcl1 and Rad2, Dna2 and DNA polymerase alpha: evidence for a multifunctional role of Mcl1 in DNA replication and repair. Curr Genet *48*, 34-43.

Verdel, A., Jia, S., Gerber, S., Sugiyama, T., Gygi, S., Grewal, S. I., and Moazed, D. (2004). RNAi-mediated targeting of heterochromatin by the RITS complex. Science *303*, 672-676.

Verreault, A., Kaufman, P. D., Kobayashi, R., and Stillman, B. (1996). Nucleosome assembly by a complex of CAF-1 and acetylated histones H3/H4. Cell *87*, 95-104.

Volpe, T. A., Kidner, C., Hall, I. M., Teng, G., Grewal, S. I., and Martienssen, R. A. (2002). Regulation of heterochromatic silencing and histone H3 lysine-9 methylation by RNAi. Science *297*, 1833-1837.

Walfridsson, J., Bjerling, P., Thalen, M., Yoo, E. J., Park, S. D., and Ekwall, K. (2005). The CHD remodeling factor Hrp1 stimulates CENP-A loading to centromeres. Nucleic Acids Res *33*, 2868-2879.

Williams, D. R., and McIntosh, J. R. (2002). *mcl1*$^{+}$, the *Schizosaccharomyces pombe* homologue of *CTF4*, is important for chromosome replication, cohesion, and segregation. Eukaryot Cell *1*, 758-773.

Williams, D. R., and McIntosh, J. R. (2005). Mcl1p is a polymerase alpha replication accessory factor important for S-phase DNA damage survival. Eukaryot Cell *4*, 166-177.

Xue, Y., Wong, J., Moreno, G. T., Young, M. K., Cote, J., and Wang, W. (1998). NURD, a novel complex with both ATP-dependent chromatin-remodeling and histone deacetylase activities. Mol Cell *2*, 851-861.

Yamada, T., Fischle, W., Sugiyama, T., Allis, C. D., and Grewal, S. I. (2005). The

nucleation and maintenance of heterochromatin by a histone deacetylase in fission yeast. Mol Cell *20*, 173-185.

Yoshida, M., Kijima, M., Akita, M., and Beppu, T. (1990). Potent and specific inhibition of mammalian histone deacetylase both in vivo and in vitro by trichostatin A. J Biol Chem *265*, 17174-17179.

Zhang, Y., Iratni, R., Erdjument-Bromage, H., Tempst, P., and Reinberg, D. (1997). Histone deacetylases and SAP18, a novel polypeptide, are components of a human Sin3 complex. Cell *89*, 357-364.

Zhang, Y., LeRoy, G., Seelig, H. P., Lane, W. S., and Reinberg, D. (1998). The dermatomyositis-specific autoantigen Mi2 is a component of a complex containing histone deacetylase and nucleosome remodeling activities. Cell *95*, 279-289.

Zhou, Y., and Wang, T. S. (2004). A coordinated temporal interplay of nucleosome reorganization factor, sister chromatin cohesion factor, and DNA polymerase alpha facilitates DNA replication. Mol Cell Biol *24*, 9568-9579.

TABLE 1. *S. pombe* strains used in this study

Strain	Genotype	Source or reference
JY746	*h⁺ leu1-32 ura4-D18 ade6-M210*	H. Mitsuzawa
TN167	*h⁺ leu1-32 ura4-D18 ade6-M210 mcl1-101*	This study
YTE18	*h⁺ leu1-32 ura4-D18 ade6-M210 mcl1Δ::ura4⁺*	This study
rad21-K1	*h⁻ leu1-32 ura4-D18 his7-366 ade6-M216 rad21-K1*	H. Okayama
swi7-H4	*h⁻ leu1-32 swi7-H4*	H. Okayama
TN310	*h⁺ leu1-32 ura4-D18 ade6-M210 swi7-H4*	This study
TN320	*h⁻ leu1-32 ura4-D18 mcl1-101 swi7-H4*	This study
TN166	*h⁻ leu1-32 ura4-D18 ade6-M210 mcl1-101*	This study
SPJ5	*h⁹⁰ leu1-32 ura4-D18 ade6-M216 swi7-1*	S. Grewal
TN663	*h⁺ leu1-32 ura4-D18 ade6-M210 swi7-1*	This study
FY1193	*h⁺ leu1-32 ura4-D18 ade6-M210 imr1L(NcoI)::ura4⁺ otr1R(SphI)::ade6⁺*	Allshire et al. (1995)
TN170	*h⁺ leu1-32 ura4-D18 ade6-M210 imr1L(NcoI)::ura4⁺ otr1R(SphI)::ade6⁺ mcl1-101*	This study
TN317	*h⁺ leu1-32 ura4-D18 ade6-M210 imr1L(NcoI)::ura4⁺ otr1R(SphI)::ade6⁺ swi7-H4*	This study
swi6Δ	*h⁺ swi6Δ::kanr*	O. Niwa
TN202	*h⁻ leu1-32 ura4-D18 ade6-M210 imr1L(NcoI)::ura4⁺ otr1R(SphI)::ade6⁺ swi6Δ::kanr*	This study
FY597	*h⁹⁰ mat3M(EcoRV)::ura4⁺ leu1-32 ura4-DS/E ade6-M210*	Allshire et al. (1995)
TN209	*h⁹⁰ mat3M(EcoRV)::ura4⁺ leu1-32 ura4-D18 ade6-M216 mcl1-101*	This study
TN318	*h⁹⁰ mat3M(EcoRV)::ura4⁺ leu1-32 ura4-D18 ade6-M210 swi7-H4*	This study
TN196	*h⁹⁰ mat3M(EcoRV)::ura4⁺ leu1-32 ura4-DS/E ade6-M216 swi6Δ::kanr*	This study
FY520	*h⁺ Ch16 m23::ura4⁺-TEL[72] leu1-32 ura4-DS/E ade6-M210 [Ch16 ade6-M216]*	Nimmo et al. (1994)
TN200	*h⁻ Ch16 m23::ura4⁺-TEL[72] leu1-32 ura4-DS/E ade6-M210 [Ch16 ade6-M216]*	This study
TN204	*h⁻ Ch16 m23::ura4⁺-TEL[72] leu1-32 ura4-DS/E ade6-M210 [Ch16 ade6-M216] mcl1-101*	This study
TN498	*h⁻ Ch16 m23::ura4⁺-TEL[72] leu1-32 ura4-D18 ade6-M210 [Ch16 ade6-M216] swi7-H4*	This study
TN199	*h⁻ Ch16 m23::ura4⁺-TEL[72] leu1-32 ura4-DS/E ade6-M210 [Ch16 ade6-M216] swi6Δ::kanr*	This study
YA869	*mat1PΔ17::LEU2 leu1-32 ura4-D18 arg3-D1 his3-D1 clr4Δ::his3⁺*	H. Iwasaki
TN458	*h⁻ leu1-32 ura4-D18 ade6-M210 imr1L(NcoI)::ura4⁺ otr1R(SphI)::ade6⁺ clr4Δ::kanr*	This study
SF02	*h⁺ leu1-32 ura4D-18 ade6-M210 polδ ts02*	T. Wang
TN915	*h⁺ leu1-32 ura4-D18 ade6-M210 imr1L(NcoI)::ura4⁺ otr1R(SphI)::ade6⁺ polδ ts02*	This study
TN916	*h⁺ leu1-32 ura4-D18 ade6-M210 imr1L(NcoI)::ura4⁺ otr1R(SphI)::ade6⁺ rad2Δ::LEU2*	This study
HK11	*h⁻ ura4-D18 leu1-32 dna2-C1*	Kang et al. (2000)
TN917	*h⁺ leu1-32 ura4-D18 ade6-M210 imr1L(NcoI)::ura4⁺ otr1R(SphI)::ade6⁺ dna2-C1*	This study
eso1-H17	*h⁻ leu1-32 eso1-H17*	H. Okayama
TN918	*h⁺ leu1-32 ura4-D18 ade6-M210 imr1L(NcoI)::ura4⁺ otr1R(SphI)::ade6⁺ eso1-H17*	This study
TN919	*h⁺ leu1-32 ura4-D18 ade6-M210 imr1L(NcoI)::ura4⁺ otr1R(SphI)::ade6⁺ ctf18Δ::kanr*	This study
TN816	*h⁺ leu1-32 ura4-D18 ade6-M210 imr1L(NcoI)::ura4⁺ otr1R(SphI)::ade6⁺ rad3Δ::kanr*	This study
TN817	*h⁺ leu1-32 ura4-D18 ade6-M210 imr1L(NcoI)::ura4⁺ otr1R(SphI)::ade6⁺ rad3Δ::kanr*	This study
TN818	*h⁺ leu1-32 ura4-D18 ade6-M210 imr1L(NcoI)::ura4⁺ otr1R(SphI)::ade6⁺ rad3Δ::kanr*	This study
SP1152	*mat1-M smt-0 mat2PΔ(Bg-Bs)::ura4⁺ ade6-M210 ura4-D18*	S. Grewal
TN480	*mat1-M smt-0 mat2PΔ(Bg-Bs)::ura4⁺ ade6-M210 ura4-D18 mcl1-101*	This study
TN482	*mat1-M smt-0 mat2PΔ(Bg-Bs)::ura4⁺ ade6-M210 ura4-D18 swi7-H4*	This study
TN488	*mat1-M smt-0 mat2PΔ(Bg-Bs)::ura4⁺ ade6-M210 ura4-D18 swi6Δ::kanr*	This study
YA679	*mat1PΔ17::LEU2 leu1-32 ura4-D18 arg3-D1 his3-D1 swi6-eyfp*	H. Iwasaki
TN266	*mat1PΔ17::LEU2 leu1-32 ura4-D18 swi6-eyfp*	This study
TN297	*mat1PΔ17::LEU2 leu1-32 ura4-D18 swi6-eyfp mcl1-101*	This study
TN299	*mat1PΔ17::LEU2 leu1-32 ura4-D18 arg3-D1 his3-D1 swi6-eyfp clr4Δ::his3⁺*	This study
TN616	*mat1PΔ17::LEU2 leu1-32 ura4-D18 swi6-eyfp* pREP42-*egfp-cnp1⁺*	This study
TN617	*mat1PΔ17::LEU2 leu1-32 ura4-D18 swi6-eyfp* pREP42-*egfp-cnp1⁺ mcl1-101*	This study
TN330	*mat1PΔ17::LEU2 leu1-32 ura4-D18 swi6-eyfp swi7-H4*	This study
TN101	*h⁺ leu1-32 ura4-D18 ade6-M210 swi6Δ::kanr*	This study
TN236	*h⁻ leu1-32 ura4-D18 ade6-M210 mcl1-101 swi6Δ::kanr*	This study
TN332	*h⁰ leu1-32 ura4-D18 mcl1-101 swi7-H4 swi6Δ::kanr*	This study
TN342	*h⁺ leu1-32 ura4-D18 ade6-M210 clr4Δ::his3⁺*	This study

TABLE 1. Continued

Strain	Genotype	Source or reference
FY336	*h⁻ leu1-32 ura4-DS/E ade6-M210 cnt1/TM(NcoI)::ura4⁺*	Allshire et al. (1995)
TN667	*h⁻ leu1-32 ura4-DS/E ade6-M210 cnt1/TM(NcoI)::ura4⁺ mcl1-101*	This study
TN668	*h⁺ leu1-32 ura4-DS/E ade6-M210 cnt1/TM(NcoI)::ura4⁺ mcl1-101*	This study
TN701	*h⁻ leu1-32 ura4-DS/E ade6-M210 cnt1/TM(NcoI)::ura4⁺ swi6Δ::kanr*	This study
TN700	*h⁺ leu1-32 ura4-DS/E ade6-M210 cnt1/TM(NcoI)::ura4⁺ swi6Δ::kanr*	This study
TN659	*h⁻ leu1-32 ura4-D18 ade6-M210 cnt1/TM(NcoI)::ura4⁺ clr4Δ::his3⁺*	This study
TN660	*h⁺ leu1-32 ura4-D18 ade6-M210 cnt1/TM(NcoI)::ura4⁺ clr4Δ::his3⁺*	This study
TN894	*h⁻ leu1-32 ura4-D18 ade6-M210 cnt1/TM(NcoI)::ura4⁺ swi7-1*	This study
TN895	*h⁻ leu1-32 ura4-D18 ade6-M210 cnt1/TM(NcoI)::ura4⁺ swi7-1*	This study
TN896	*h⁺ leu1-32 ura4-D18 ade6-M210 cnt1/TM(NcoI)::ura4⁺ swi7-1*	This study
TN827	*h⁻ leu1-32 ura4-D18 ade6-M210 cnt1/TM(NcoI)::ura4⁺ swi7-H4*	This study
TN828	*h⁻ leu1-32 ura4-DS/E ade6-M210 cnt1/TM(NcoI)::ura4⁺ swi7-H4*	This study
TN829	*h⁺ leu1-32 ura4-D18 ade6-M210 cnt1/TM(NcoI)::ura4⁺ swi7-H4*	This study
TN933	*h⁺ leu1-32 ura4-D18 ade6-M210* pREP42-EYFP-*cnp1⁺*	This study
TN934	*h⁺ leu1-32 ura4-D18 ade6-M210* pREP42-EYFP-*cnp1⁺ mcl1-101*	This study
TN705	*h⁺ leu1-32 ura4-D18 ade6-M210 cnp1-FH::kanMX6*	This study
TN928	*h⁺ leu1-32 ura4-D18 ade6-M210 mis6-GFP::kanMX6*	This study
TN936	*h⁺ leu1-32 ura4-D18 ade6-M210 mis6-GFP::kanMX6 mcl1-101*	This study
TN921	*h⁺ leu1-32 ura4-D18 ade6-M210 ams2Δ::kanr*	This study
TN711	*h⁺ leu1-32 ura4-D18 ade6-M210 hrp1Δ::kanr*	This study
TN371	*h⁺ leu1-32 ura4-D18 ade6-M210 chp1-GFP::kanMX6*	This study
TN423	*h⁺ leu1-32 ura4-D18 ade6-M210 chp1-GFP::kanMX6 mcl1-101*	This study
TN434	*mat1-M smt-0 leu1-32 ura4-D18 ade6-M210 chp1-GFP::kanMX6 clr4Δ::his3⁺*	This study
TN477	*mat1PΔ17 leu1⁻ ura4⁻ ade6⁻ imr1L(NcoI)::ura4⁺ otr1R(SphI)::ade6⁺ swi6-eyfp*	This study
TN479	*mat1PΔ17 leu1⁻ ura4⁻ ade6⁻ imr1L(NcoI)::ura4⁺ otr1R(SphI)::ade6⁺ swi6-eyfp mcl1-101*	This study
TN490	*mat1PΔ17 leu1⁻ ura4⁻ ade6⁻ imr1L(NcoI)::ura4⁺ otr1R(SphI)::ade6⁺ swi6-eyfp clr4D::his3⁺*	This study
TN658	*h⁺ leu1-32 ura4-D18 ade6-M210 rad21-myc::kanMX6*	This study
TN867	*h⁺ leu1-32 ura4-D18 ade6-M210 rad21-myc::kanMX6 mcl1-101*	This study
TN889	*h⁺ leu1-32 ura4-D18 ade6-M210 rad21-myc::kanMX6 swi7-H4*	This study
TN870	*h⁺ leu1-32 ura4-D18 ade6-M210 rad21-myc::kanMX6 swi6Δ::kanr*	This study
GBY572	*h⁺ ura4-D18 ade6-M216 leu1::(dfp1⁺-6his3HA leu1⁺) dfp1-D1*	G. Brown
AFY7	*h⁺ ura4-D18 ade6-M216 leu1::(dfp1$_{1-376}$-6his3HA leu1⁺) dfp1-D1*	G. Brown
TN886	*h⁺ ura4⁻ ade6⁻ leu1::(dfp1$_{1-376}$-6his3HA leu1⁺) dfp1-D1 cnt1/TM(NcoI)::ura4⁺*	This study
TN887	*h⁺ ura4⁻ ade6⁻ leu1::(dfp1$_{1-376}$-6his3HA leu1⁺) dfp1-D1 cnt1/TM(NcoI)::ura4⁺*	This study
TN888	*h⁺ ura4⁻ ade6⁻ leu1::(dfp1$_{1-376}$-6his3HA leu1⁺) dfp1-D1 cnt1/TM(NcoI)::ura4⁺*	This study
TN583	*h⁺ leu1-32 ura4-D18 ade6-M210 sir2Δ::ura4⁺*	This study
TN582	*h⁺ leu1-32 ura4-D18 ade6-M210 hst4Δ::kanr*	This study
TN639	*h⁺ leu1-32 ura4-D18 ade6⁻ mcl1-101 sir2Δ::ura4⁺*	This study
TN642	*h^{90} leu1-32 ura4-D18 ade6⁻ mcl1-101 sir2Δ::ura4⁺*	This study
TN633	*h⁻ leu1-32 ura4-D18 ade6⁻ mcl1-101 hst4Δ::kanr*	This study
TN634	*h⁺ leu1-32 ura4-D18 ade6⁻ mcl1-101 hst4Δ::kanr*	This study

TABLE 2. Oligonucleotide primers used in this study

Purpose	Location	Name of primer	Sequence (5'-3')
RT-PCR	*act1*	act1-F1	GATAATGGCTCTGGTATGTG
		act1-R1	CTTTTGTCCCATACCTACCA
	ura4	ura4-3	GGCTCATATCACAAATTGCC
		ura4-4	CGTCCCAAAGGTAAACCAAC
ChIP	*ade6-1*	ade6-F	GGCCAAGAGTTTGGTTATCC
		ade6-R	TAAAGCGGACGATCACCAAG
	ade6-2	ade6-436F	CGACCACATTGGCTTACGACGGTCG
		ade6-489R	CATAAAGCGGACGATCACCAAG
	lys1	lys1-1	CCAACAGATTATAGTCGTCC
		lys1-2	CTTGAGCAGCAACATAAACC
	cnt-1	cnt-a	TCACGTCCCGGTTAGTTTAC
		cnt-c	TCATAATACAGGAGGAATTGTG
	cnt-2	cnt-TM1-a	CACAACCATAAAGCCGTATTC
		cnt-TM1-b	AACCCCGTTGTTAAACATATG
	cnt-3	cnt-a	TCACGTCCCGGTTAGTTTAC
		cnt-b	GAATTAAATATGTTTTACAACGTG
	imr256	imr256-2	AGCATTGCCAGCTCATATTA
		imr256-3	GAGCTTATGGAAAAAATGTTTG
	imr195	imr195-3	GTATCGCAACGATTTGAACTG
		imr195-4	CATAACCACCACCATGCTC
	dg	dg223-3	TGGTAATACGTACTAGCTCTCG
		dg223-4	CTAATTCATGGGTGATTGATG
	dh	dh383-2	TTCTGAATAATTGGGATCGC
		dh383-3	AGGAAGATTTCACTCATACCTACC
	mat2P	mat2P-3	CTTTGTTCCCTCTTTCTTTG
		mat2P-4	TTAGTGATATAAAACGCCCACA
	cenH	matK-3	GAAATATGGCTCCATTGGTTG
		matK-4	CGCCATCCATTTTGGTTGTG
	TEL	TEL-FW3	GTAACAATGTAGAATAAGGAGC
		TEL-RV2	TGGGGGCATTTTATATATGTGA
	ura4 (ChIP)	ura4-1	TTGCTTCTTGGGCTCATATC
		ura4-2	CCTTTGGAAGACATTTCAGC
MNase	*cnt1*	cnt1-F1	ATGCGAATTCAACTCTGTTTATTAA
		cnt1-R1	TAGAAAGCTTTAATTATTCGTTCG
	imr1L	imr1L-F1	ATGTGCATGCTATATTGGTATTG
		imr1L-R1	TACCAAGCTTTACTAAATGTAAGAA
	otr1L	otr1L-F1	CAGGGCATGCTTAGCAAGTAC
		otr1L-R1	ATTTAAGCTTTCCCTTGAATTTTC

TABLE 3. Genetic interactions with *mcl1-101*

Mutation	Function	Interaction
DNA replication	-	-
swi7-1	DNA polymerase α catalytic subunit	Synthetically lethal at 25 ºC
swi7-H4	DNA polymerase α catalytic subunit	Synthetically lethal at 30 ºC / Synergistic TBZ sensitivity
Heterochromatin	-	-
swi6Δ	HP1 homologue	Synergistic TBZ sensitivity
clr4Δ	Histone H3 Lys9 methyltransferase	Synthetic growth defect or lethal
Sister chromatid cohesion	-	-
rad21-K1	Cohesin subunit	Synthetically lethal at 25 ºC
Chromatin remodeling factor	-	-
hrp1Δ	Heterochromatin assembly, Cnp1 loading	Synthetically lethal at 34 ºC
hrp3Δ	Heterochromatin assembly	Synthetically lethal at 34 ºC
pob3-L73R	Yeast FACT complex	Synthetically lethal at 30 ºC
Kinetochore	-	
cnp1-FH	Histone H3 variant	Synthetically lethal at 25 ºC
ams2Δ	GATA factor, Cnp1 loading	Synthetically lethal at 25 ºC
Histone deacetylase	-	-
sir2Δ	Histone H3 Lys9 deacetylation	Synergistic TSA sensitivity
hst4Δ	Histone deacetylation	Suppression of slow growth of *hst4Δ*

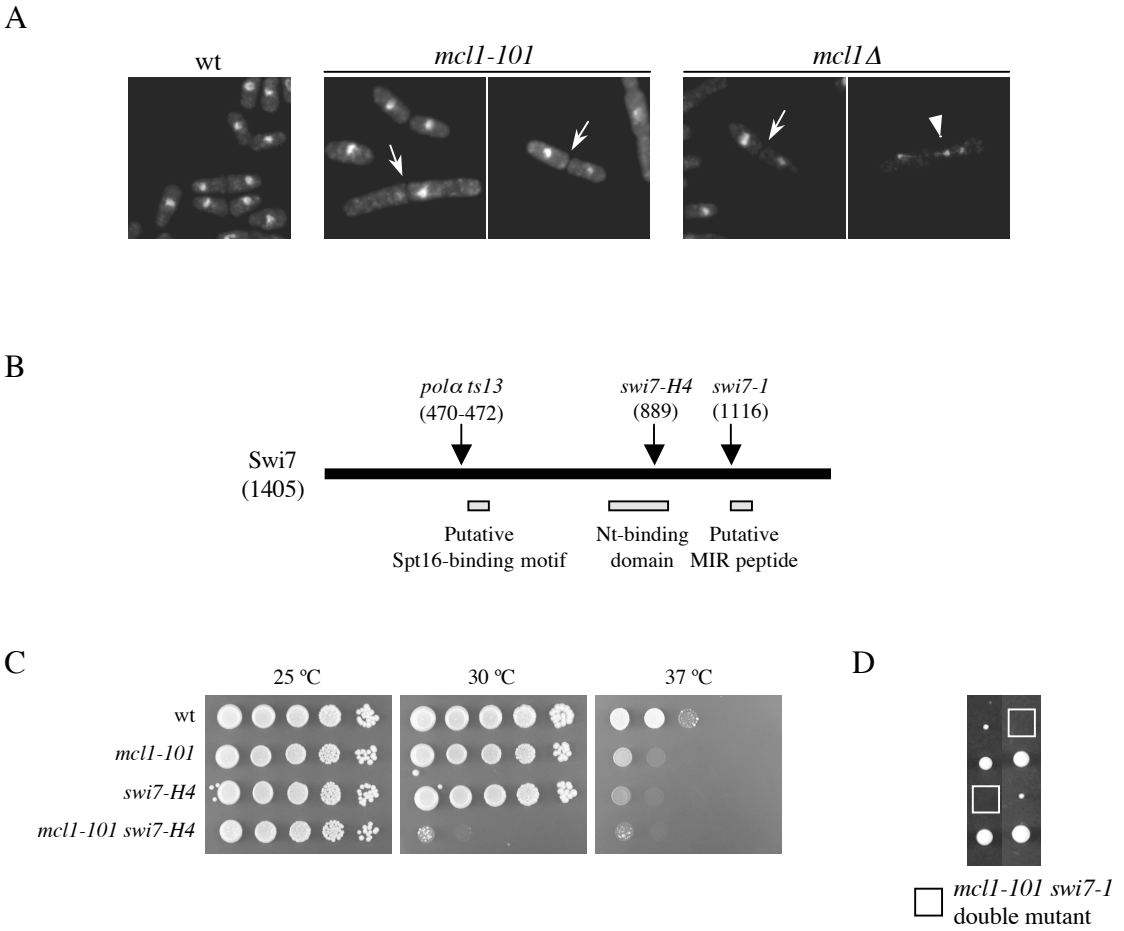

FIG. 1. Aberrant mitosis of *mcl1* mutant cells and genetic interactions between Mcl1 and Swi7. (A) Unequal chromosome segregation and lagging chromosomes are observed in Mcl1-deficient cells. Cells of wild-type (TN154) and *mcl1-101* (TN167) were incubated at 37 ºC for 6 hr before fixation. Cells of *mcl1Δ* (YTE18) were prepared at 25 ºC. Fixed cells were stained with DAPI and observed under ECLIPSE E800 (Nikon). Arrows indicate unequal segregation and the arrowhead represents lagging chromosomes. (B) Location of *swi7* mutations are shown. The *polα ts13* mutation is located in 6 a.a. upstream of a putative binding motif with chromatin remodeling factor, Spt16 (Zhou and Wang, 2004). The *swi7-H4* mutation resides in the nucleotide (Nt) binding motif (Ahmed et al., 2001). The *swi7-1* mutation is located in 13 a.a. upstream of putative MOD1-interacting region (MIR) peptide, which is considered to interact with chromo-shadow domain in HP1 protein (Nakayama et al., 2001). (C) The *mcl1-101 swi7-H4* double mutant is viable, but shows a reduced maximum temperature for growth. Ten-fold serial dilutions of wt (JY746), *mcl1-101* (TN167), *swi7-H4* (TN310), and *mcl1-101 swi7-H4* (TN320) strains were plated onto YES plates and incubated at indicated temperature for 3 days (D) The *mcl1-101* mutation is synthetic lethal with the *swi7-1* mutation. The *mcl1-101* (TN166) and *swi7-1* (TN663) mutants were crossed, and the produced asci were dissected and incubated at 25 ºC (tetrad analysis).

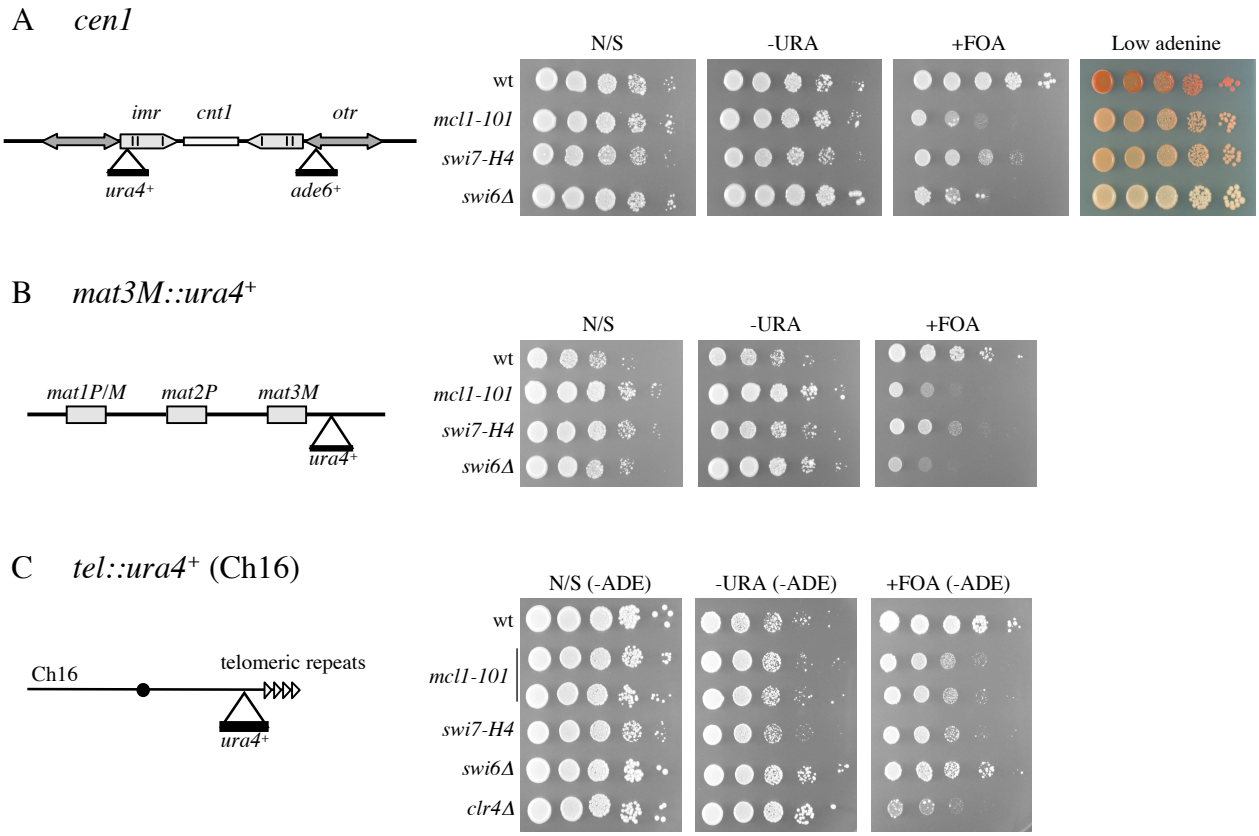

D *cen1* transcript (*imr::ura4*+)

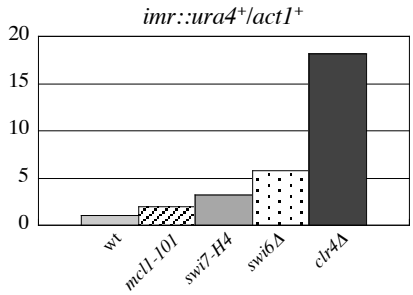

FIG. 2. The *mcl1-101* mutant alleviates transcriptional gene silencing at centromere, mating type region, and telomere. (A) Left: schematic diagram of marker genes inserted at *otr* and *imr* of *cen1*. Note that *ura4*+ gene resides on the heterochromatin domain, which is defined as outside of tRNA genes (vertical lines in *imr*) . Right: Ten-fold serial dilutions of wt (FY1193), *mcl1-101* (TN170), *swi7-H4* (TN317), and *swi6Δ* (TN202) strains were plated onto non-selective EMM (N/S), EMM lacking uracil (-URA) which shows the expression of *ura4*+ reporter gene, EMM containing 5-FOA (FOA) which counterselects *ura4*+-expressing cells, and YE (Low adenine) on which the expression of *ade6*+ reporter gene changes colony color from red to white. Plates were incubated at 30 ºC for 4 days. (B) Left: schematic diagram of the marker gene inserted at centromere-distal side of *mat3M* locus. Right: Ten-fold serial dilutions of wt (FY597), *mcl1-101* (TN209), *swi7-H4* (TN318), and *swi6Δ* (TN196) strains were plated onto non-selective EMM (N/S), EMM lacking uracil (-URA) and EMM containing 5-FOA (FOA). Plates were incubated at 32 ºC for 4 days. (C) Left: schematic diagram of the marker gene inserted adjacent to telomeric repeats on non-essential mini-chromosome (Ch16). Right: Ten-fold serial dilutions of wt (TN200), *mcl1-101* (TN204), *swi7-H4* (TN498), and *swi6Δ* (TN199) strains were plated onto non-selective EMM (N/S), EMM lacking uracil (-URA) and EMM containing 5-FOA (FOA). Note that all plates lack adenine to select cells harboring non-essential mini chromosome, and Glucose are replaced with Glutamate to aid growth of these strains. Plates were incubated at 34 ºC for 4 days. (D) Transcripts from *imr::ura4*+ were quantified by real-time RT-PCR. Transcripts of *imr::ura4*+ were normalized by that of *act1*+ as a control. Values indicate fold changes compared to wt (1.0). Cells of wt (JY746), *mcl1-101* (TN167), *swi7-H4* (TN317), *swi6Δ* (TN202), and *clr4Δ* (TN458) were grown at 32 ºC and used for total RNA preparation.

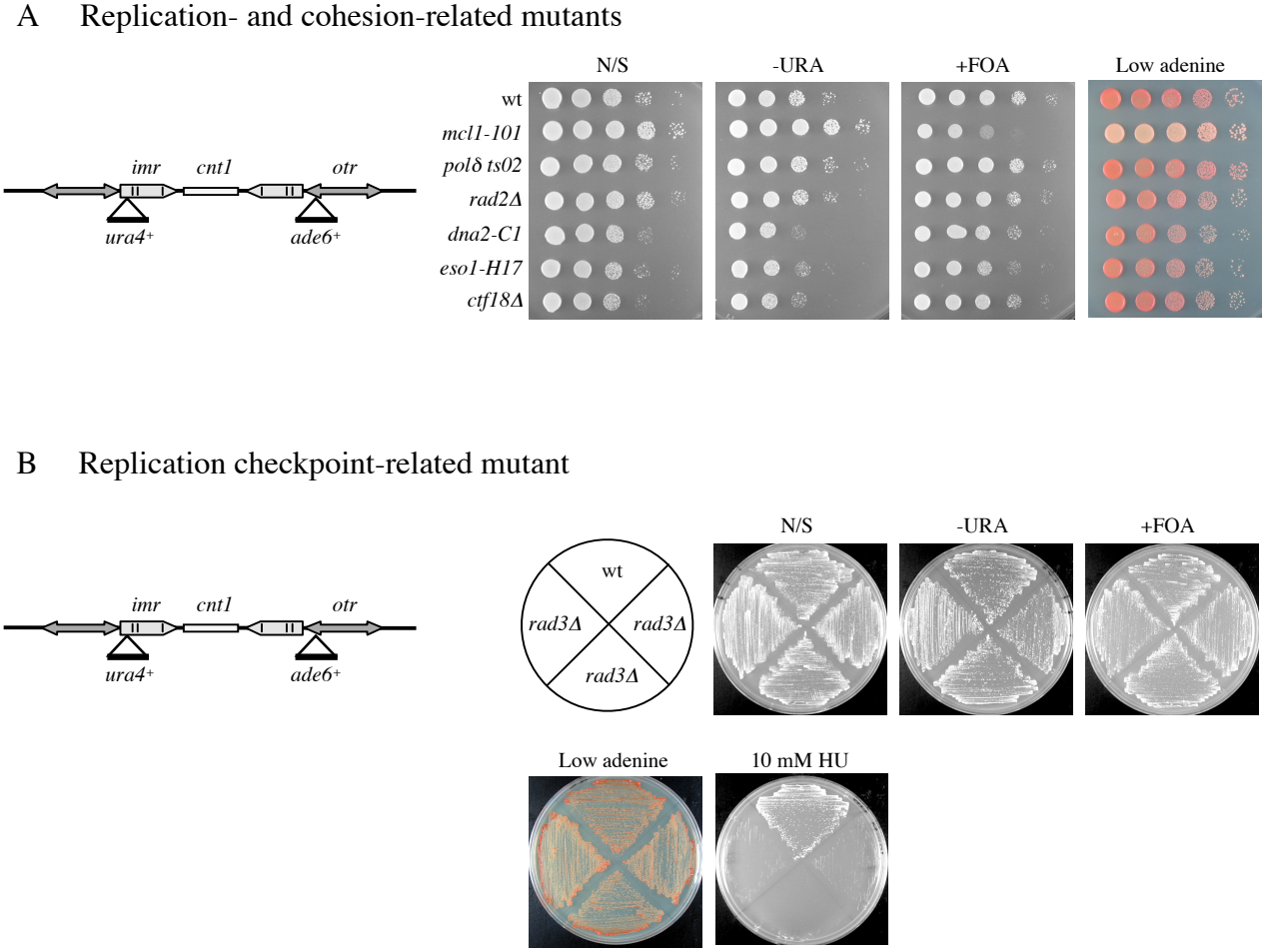

FIG. 3. Transcriptional gene silencing at centromere is not alleviated in other replication-, cohesion-, and checkpoint-related mutants. (A) Left: schematic diagram of marker genes inserted at *otr* and *imr* of *cen1*. Right: ten-fold serial dilutions of wt (FY1193), *mcl1-101* (TN170), *polδ ts02* (TN915), *rad2Δ* (TN916), *dna2-C1* (TN917), *eso1-H17* (TN918), and *ctf18Δ* (TN919) strains were plated onto non-selective EMM (N/S), EMM lacking uracil (-URA), EMM containing 5-FOA (FOA), and YE (Low adenine). Plates were incubated at 25 ºC for 4 days. (B) Left: schematic diagram of marker genes inserted at *otr* and *imr* of *cen1*. Right: cells of wt (FY1193) and *rad3*Δ (TN816, TN817, and TN818) were streaked onto EMM (N/S), EMM lacking uracil (-URA), EMM containing 5-FOA (FOA), YE (Low adenine), and YES containing 10 mM hydroxy urea (HU) to confirm replication checkpoint defect of *rad3Δ* mutants. Plates were incubated at 30 ºC for 4 days.

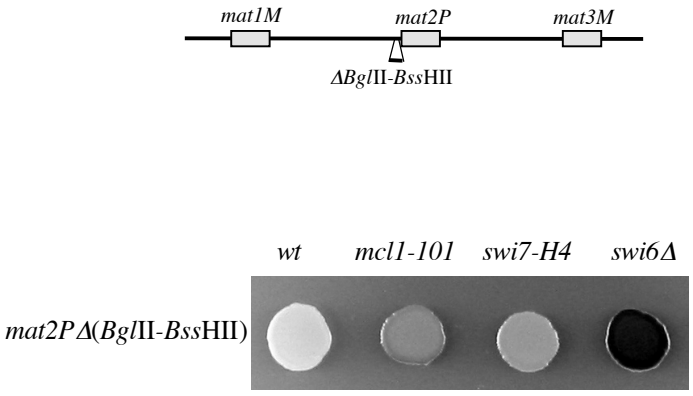

FIG. 4. The *mcl1-101* haploid cell undergoes aberrant meiosis knows as "haploid meiosis". Top: schematic diagram of *mat* loci. In wild-type cell, only *mat1M* is transcriptionally active while *mat2P* and *mat3M* are silent due to heterochromatin. Bottom: haploid cells of wt (SP1152), *mcl1-101* (TN480), *swi7-H4* (TN482), and swi6Δ (TN488) were spotted onto sporulation media (SPA), incubated at 30 ºC, and stained with iodine vapor. Spores produced in aberrant meiosis turns brown because the starch-like substance in spores is stained by iodine vapor. All strains are *mat2PΔ*(*Bgl*II-*Bss*HII) background, in which *BglII-BssHII* fragment on the centromere proximal side is deleted.

A

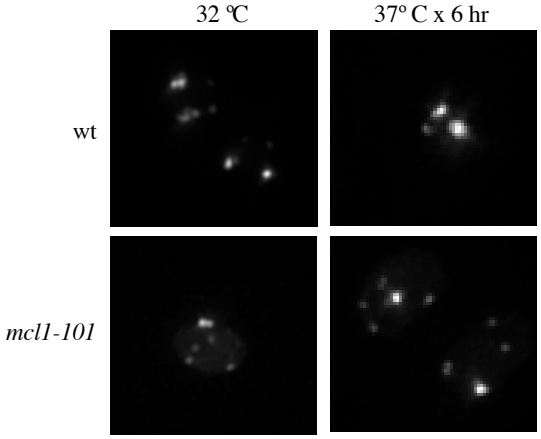

B

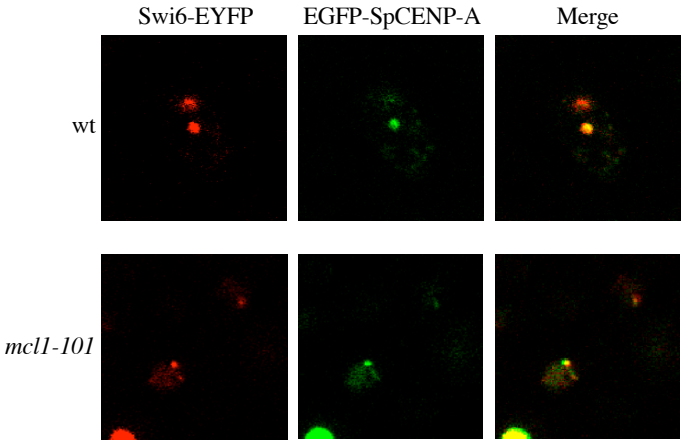

FIG. 5. Fluorescent microscopy of Swi6-EYFP in the *mcl1-101* mutant. (A) Cells expressing Swi6-EYFP in the wt (TN266) and *mcl1-101* (TN297) background were incubated at semi-permissive temperature (32 ℃, left) or restrictive temperature (37 ℃ for 6 hr, right), and observed under DeltaVision™ (Applied Precision). (B) Cells expressing both Swi6-EYFP (left, red) and EGFP-SpCENP-A (middle, green) in the wt (TN616) and *mcl1-101* (TN617) background were observed under FV1000 laser confocal microscope (Olympus). Merged images are also shown (right, yellow).

A

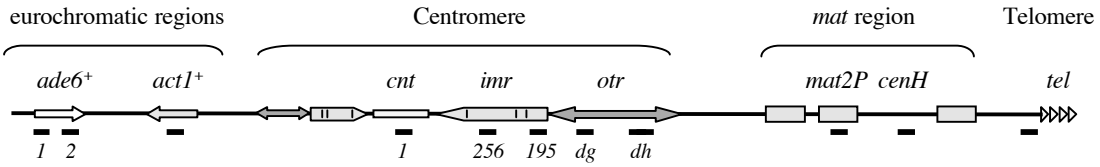

B

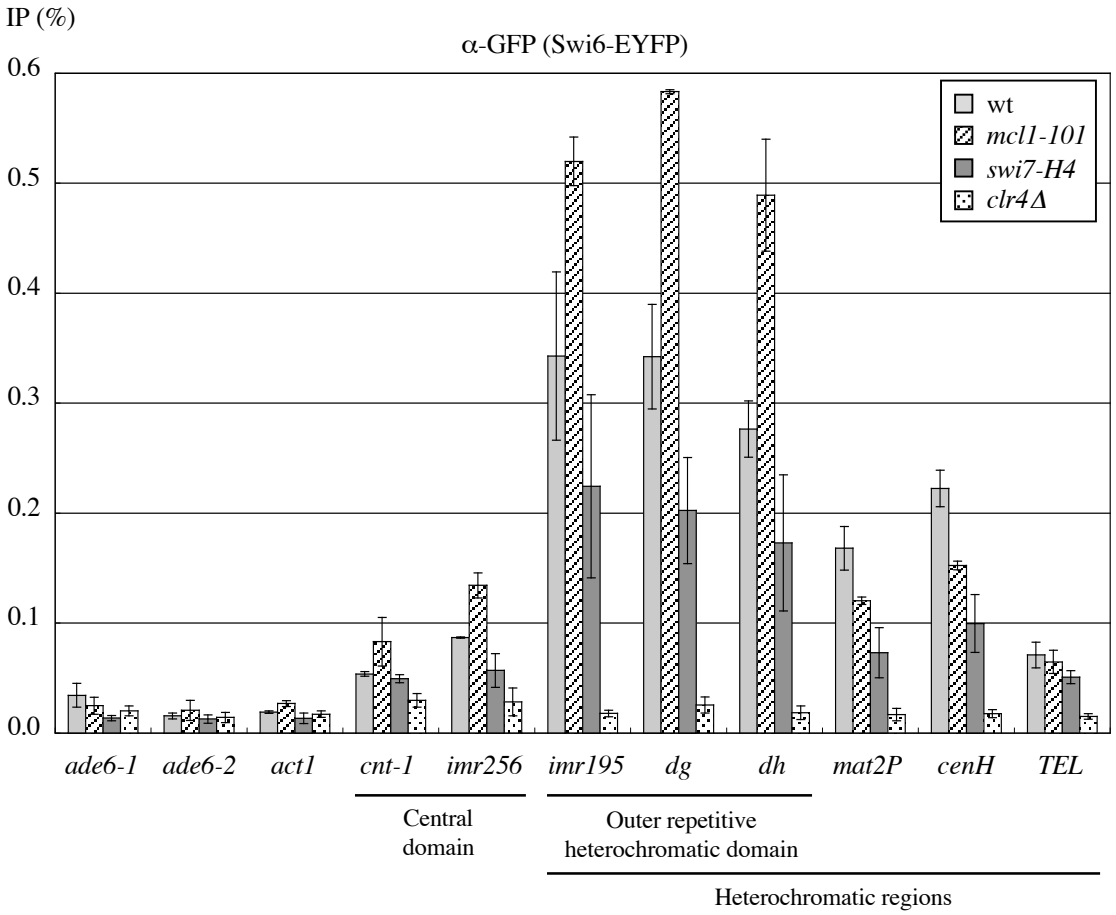

FIG. 6. Chromatin association of Swi6-EYFP in the *mcl1-101* mutant. (A) Schematic diagrams of *S. pombe* chromosome and locations of PCR primers used in the chromatin immunoprecipitation assay (horizontal lines). (B) ChIP was performed using α-GFP antibody for cells expressing Swi6-EYFP in the wt (TN266), *mcl1-101* (TN297), *swi7-H4* (TN330) and *clr4Δ* (TN299) background. Precipitated DNA was quantified by real-time PCR using LightCycler (Roche). The average ratios of immunoprecipitated DNA to input DNA obtained from two repetitions are shown. All strains were incubated at semi-permissive temperature for the *mcl1-101* (32 ºC).

A

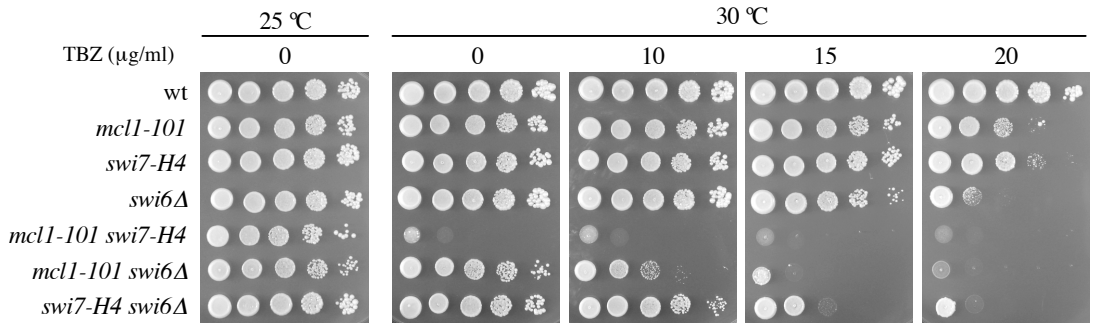

B

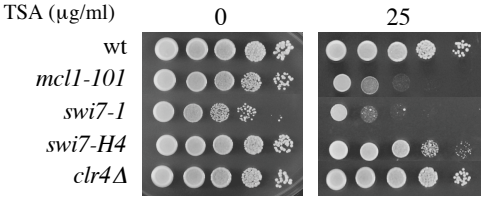

FIG. 7. Mcl1 and Swi7 might function in the Swi6-Clr4 independent pathway. (A) The *mcl1-101* and *swi7-H4* mutants are synergistically sensitive to microtubule (MT) destabilizing drug, TBZ, in combination with the *swi6Δ* mutation. Ten-fold serial dilutions of wt (JY746), *mcl1-101* (TN167), *swi7-H4* (TN310), *swi6Δ* (TN101), *mcl1-101 swi7-H4* (TN320), *mcl1-101 swi6Δ* (TN236), and *swi7-H4 swi6Δ* (TN332) strains were plated onto YES containing indicated concentration of TBZ and incubated for 3 day. Note that mutants sensitive to this drug are considered to be defective in MT-kinetochore attachment. (B) The *mcl1-101* and *swi7* mutants, but not *clr4Δ* mutant, are sensitive to histone deacetylase inhibitor, Trichostatin A (TSA). Ten-fold serial dilutions of wt (JY746), *mcl1-101* (TN167), *swi7-1* (TN663), *swi7-H4* (TN310), and *clr4Δ* (TN342) strains were plated onto YES containing indicated concentration of TSA and incubated at 30 ºC for 3 day.

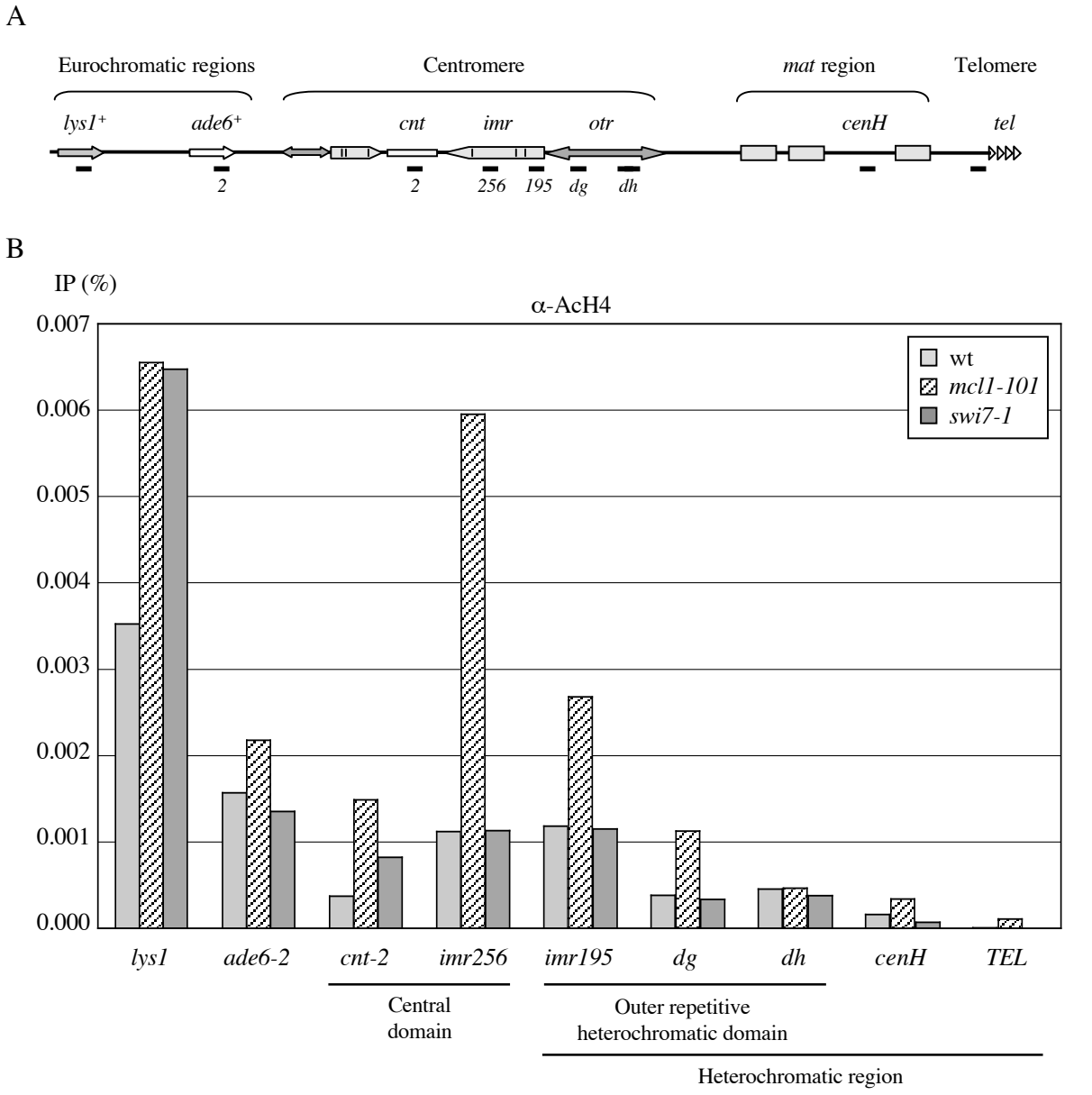

FIG. 8. The level of histone H4 acetylation in the *mcl1-101* mutant. (A) Schematic diagrams of *S. pombe* chromosome and locations of PCR primers used in chromatin immunoprecipitation assay (horizontal lines). (B) ChIP was performed using α-acetyl histone H4 (2-19) antiserum (α-AcH4) for wt (TN154), *mcl1-101* (TN167), and *swi7-1* (TN663). Precipitated DNA was quantified by real-time PCR using LightCycler (Roche). The ratios of immunoprecipitated DNA (α-AcH4 sample minus no antibody sample) to input DNA obtained from one repetition are shown. All strains were incubated at restrictive temperature for the *mcl1-101* (36 ºC) for 6 hr before fixation. (C) Acetylation level of bulk histone in wt (TN154) and *mcl1-101* (TN167) strains, which were incubated at restrictive temperature (37 ºC) for 6 hr before extraction. Two-fold dilutions of total protein extracts were separated and examined by western blotting using α-acetyl histone H4 (2-19) antiserum (α-AcH4) and α-Cdc2 (PSTAIRE) as a loading control.

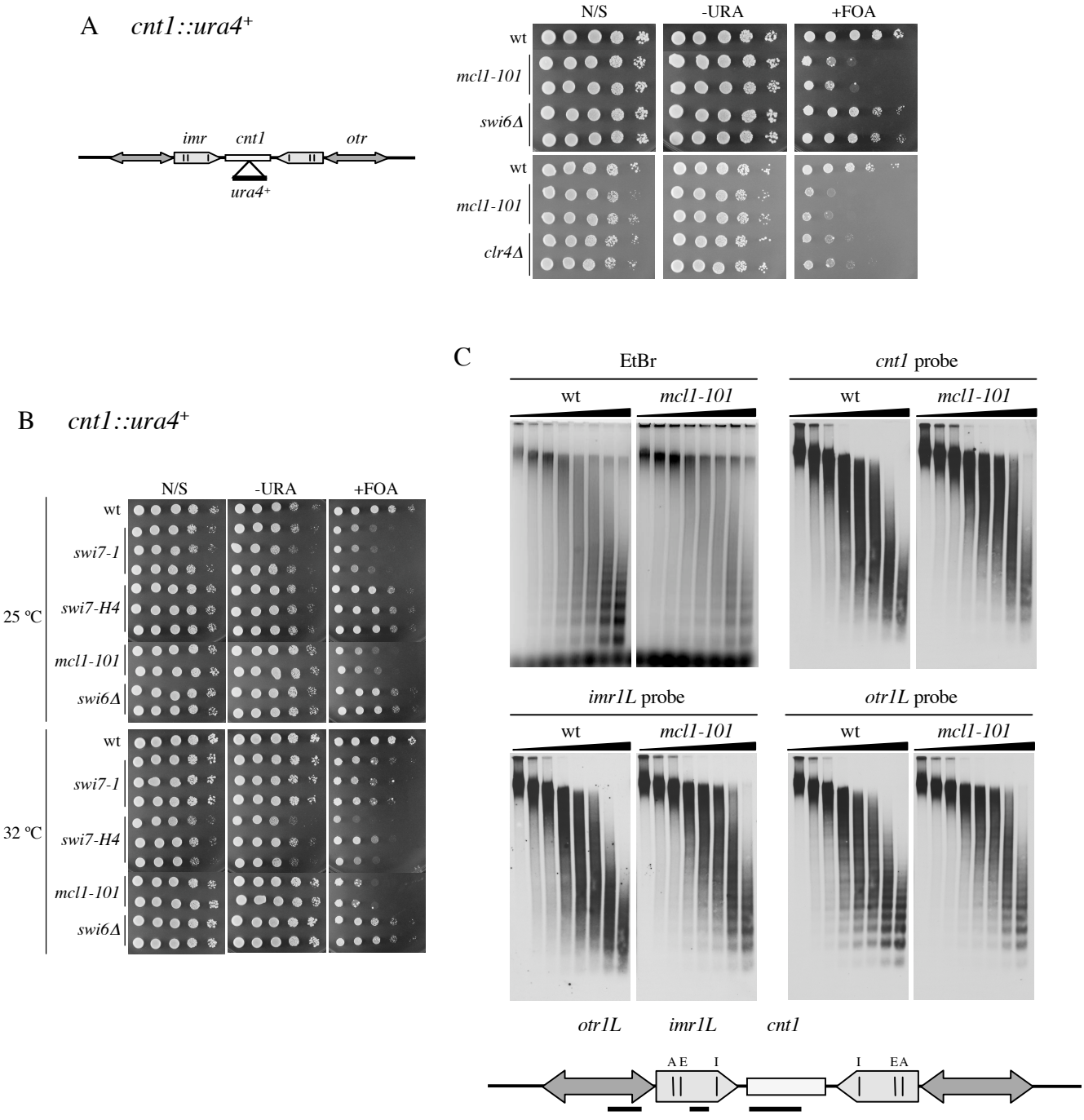

FIG. 9. Specialized chromatin structure of central domain is disrupted in the *mcl1-101* mutant. (A) Left: schematic diagram of the marker gene inserted at *cnt* of *cen1* (*cnt1*). Right: Ten-fold serial dilutions of wt (FY336), *mcl1-101* (TN667, TN668), *swi6Δ* (TN701, TN700), and *clr4Δ* (TN659. TN660) strains were plated onto non-selective EMM (N/S), EMM lacking uracil (-URA), EMM containing 5-FOA (FOA). Plates were incubated at 30 ºC for 4 days. (B) Ten-fold serial dilutions of wt (FY336), *swi7-1* (TN894-896), *swi7-H4* (TN827-829), *mcl1-101* (TN667, TN668), and *swi6Δ* (TN701, TN700) strains were plated onto non-selective EMM (N/S), EMM lacking uracil (-URA), EMM containing 5-FOA (FOA). Plates were incubated at indicated degree for 4 day. (C) Top: chromatin was prepared from cultures of wt (JY746) and *mcl1-101* (TN167) incubated at 36 ºC for 6 hr, and subjected to MNase digestion. DNA was extracted, separated on 1.5% agarose gel, and subjected to Southern hybridization. Ethidium bromide (EtBr)-stained images are also shown. Bottom: probes used in the hybridization were represented (horizontal line). Vertical lines in *imr* indicate tRNA genes; A: $tRNA^{Ala}$, E: $tRNA^{Glu}$, I: $tRNA^{Ile}$. Note that $tRNA^{Ala}$ and $tRNA^{Glu}$ defines a transition zone between central domain (*cnt* and inner part of *imr*) and outer repetitive heterochromatic domain (*otr* and outer part of *imr*).

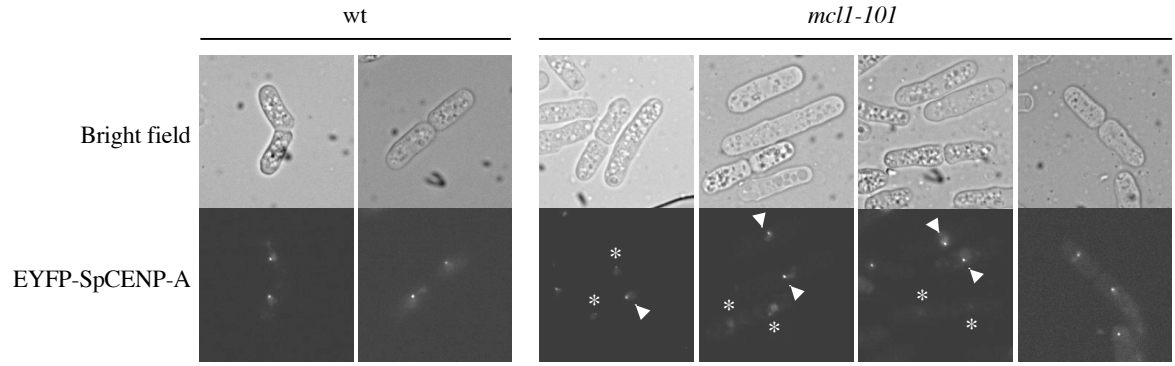

FIG. 10. SpCENP-A loading to kinetochore is diminished in separating *mcl1-101* cells. Cells expressing EYFP-SpCENP-A under control of thiamine-repressible promoter in the wt (TN933) and *mcl1-101* background (TN934) were nitrogen-starved to synchronize at G1 phase in the absence of thiamine (inducible) and released at 37 ºC for 6 hr. EYFP-SpCENP-A localization was observed under ECLIPSE E800 (Nikon). Arrowheads indicate normal EYFP-SpCENP-A signal similar to the wild-type, whereas asterisks represent weak or dispersed signal in the *mcl1-101* cells. The most right. The rightmost image represents normal localization of EYFP-SpCENP-A in *mcl1-101* cells. For the wild-type, only separating cells are shown.

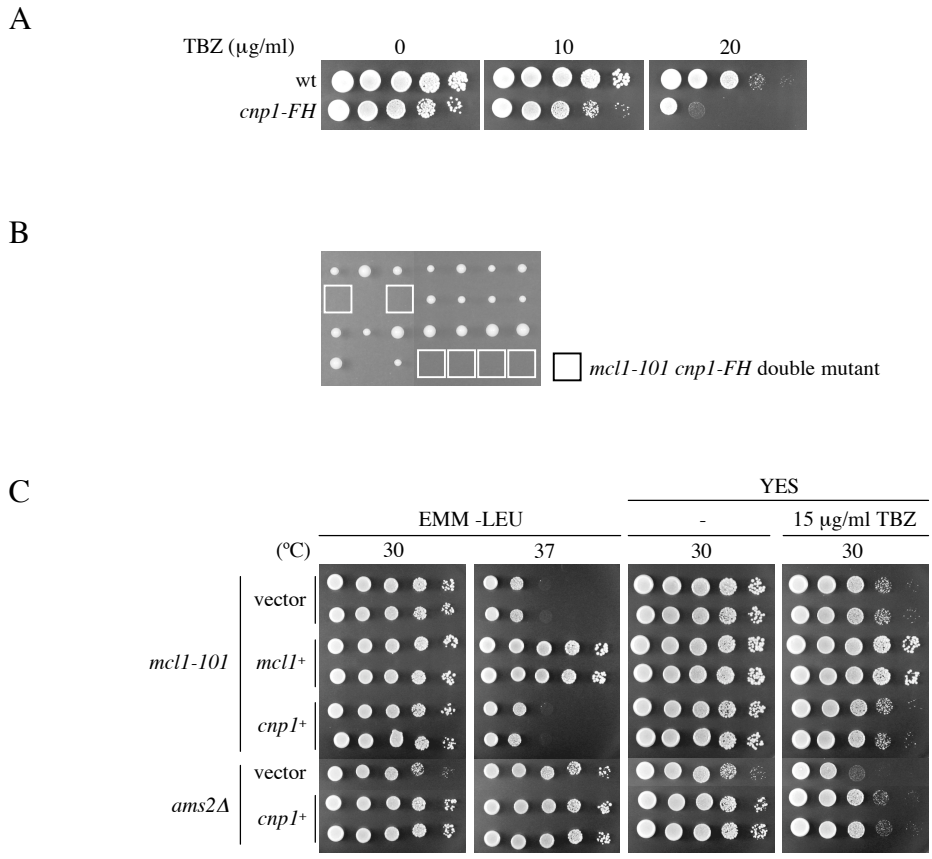

FIG. 11. Genetic interactions of Mcl1 with SpCENP-A (Cnp1). (A) The C-terminally 3xFLAG 6xHis-tagged *cnp1* strain (*cnp1-FH)* is sensitive to TBZ. Ten-fold serial dilutions of wt (JY746) and *cnp1-FH* (TN705) strains were plated onto YES containing indicated concentration of TBZ and incubated for 3 day at 30 ºC. (B) The *mcl1-101* mutation is synthetic lethal with *cnp1-FH*. The *mcl1-101* (TN166) and *cnp1-FH* (TN705) mutants were crossed, and the produced asci were dissected and incubated at 30 ºC (tetrad analysis). (C) Neither temperature sensitivity nor TBZ sensitivity of the *mcl1-101* strain is suppressed by overexpression of SpCENP-A. Ten-fold serial dilutions of *mcl1-101* (TN167) strains harboring a *LEU2*-carrying multi-copy plasmid pSP102 (vector,), pSP102-*mcl1*$^+$ (*mcl1*$^+$), and pSP102-*cnp1*$^+$ (*cnp1*$^+$) were plated onto EMM lacking leucine and YES containing indicated concentration of TBZ. As a control, the *ams2Δ* (TN920) strains harboring pSP102 (vector) and pSP102-*cnp1*$^+$ (*cnp1*$^+$) were also included. Plates were incubated at indicated temperature for 3 days (EMM) or 4 days (YES).

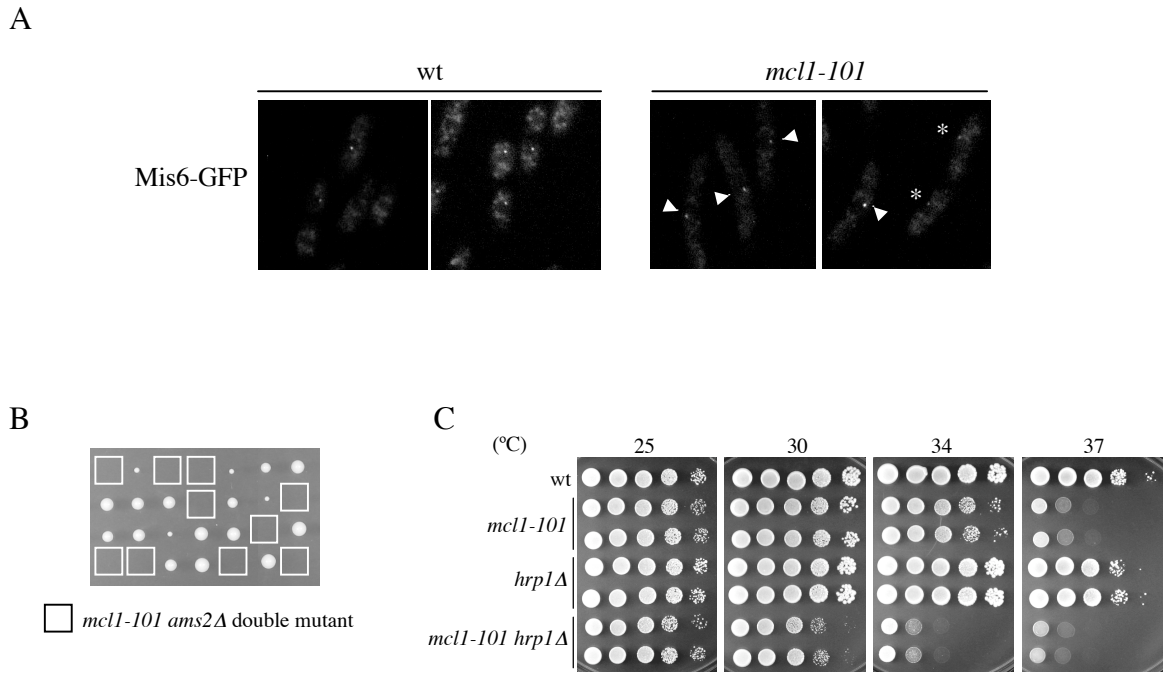

FIG. 12. Relationships between Mcl1 and two SpCENP-A loading pathways characterized so far. (A) Mis6 localization in *mcl1-101* cells. Cells expressing Mis6-GFP from its endogenous locus in the wt (TN928) and *mcl1-101* (TN936) background were incubated for 6 hr at restrictive temperature, 37 ºC, and observed under ECLIPSE E800 (Nikon). Arrowheads and asterisks indicate Mis6-GFP spots in cells with one nucleus (possibly G2 phase) and in separating cells (S phase), respectively. (B) The *mcl1-101* mutation is synthetic lethal with *ams2Δ*. The *mcl1-101* (TN166) and *ams2Δ* (TN921) mutants were crossed, and the produced asci were dissected and incubated at 30 ºC (tetrad analysis). (C) The *mcl1-101 hrp1Δ* double mutants is viable, but shows reduced maximum temperature for growth. The *mcl1-101* (TN166) and *hrp1Δ* (TN711) mutants were crossed, and the produced asci were dissected. Ten-fold serial dilutions of segregants from two tetra-type crosses were plated onto YES and incubated for 3 day at indicated temperature.

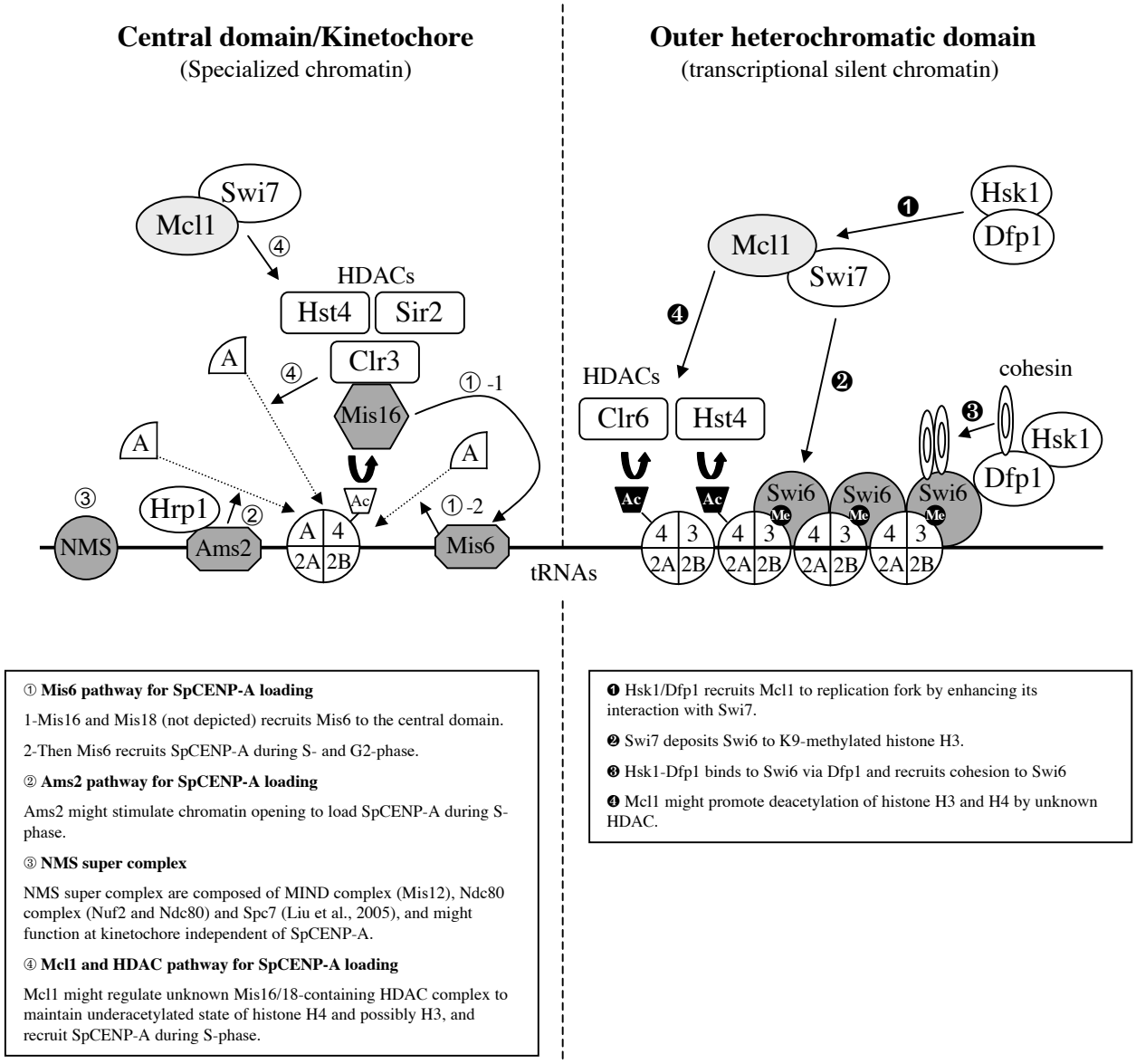

① **Mis6 pathway for SpCENP-A loading**

1-Mis16 and Mis18 (not depicted) recruits Mis6 to the central domain.

2-Then Mis6 recruits SpCENP-A during S- and G2-phase.

② **Ams2 pathway for SpCENP-A loading**

Ams2 might stimulate chromatin opening to load SpCENP-A during S-phase.

③ **NMS super complex**

NMS super complex are composed of MIND complex (Mis12), Ndc80 complex (Nuf2 and Ndc80) and Spc7 (Liu et al., 2005), and might function at kinetochore independent of SpCENP-A.

④ **Mcl1 and HDAC pathway for SpCENP-A loading**

Mcl1 might regulate unknown Mis16/18-containing HDAC complex to maintain underacetylated state of histone H4 and possibly H3, and recruit SpCENP-A during S-phase.

❶ Hsk1/Dfp1 recruits Mcl1 to replication fork by enhancing its interaction with Swi7.

❷ Swi7 deposits Swi6 to K9-methylated histone H3.

❸ Hsk1-Dfp1 binds to Swi6 via Dfp1 and recruits cohesion to Swi6

❹ Mcl1 might promote deacetylation of histone H3 and H4 by unknown HDAC.

FIG. 13. Mcl1 is involved in maintenance of two distinct domain structures of centromere, possibly by regulating histone deacetylation. Constitutively-associated, non-histone chromatin proteins are shown by dark grey figures. Abbreviations are as follows; A: SpCENP-A, 3: histone H3, 4: histone H4, 2A:histone H2A, 2B: histone H2B, Me: methylation, Ac: acetylation.

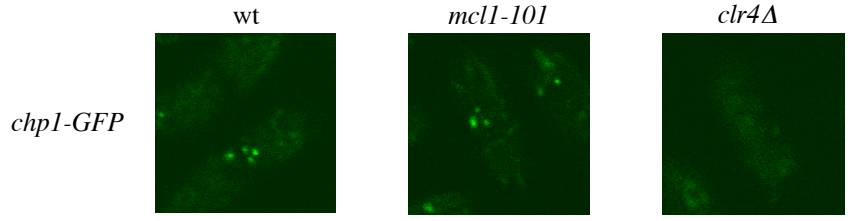

FIG. S1. Fluorescent microscopy of Chp1-GFP in the *mcl1-101* mutant. (A) Localization of Chp1-GFP in the wt (TN371), *mcl1-101* (TN423), and *clr4Δ* (TN434) background was observed at 25 ºC under FV1000 laser confocal microscope (Olympus). In the wild type, Chp1-GFP forms 1-4 spots in the nucleus while Chp1-GFP is dispersed within the nucleus in the *clr4Δ* mutant.

A *cen1*

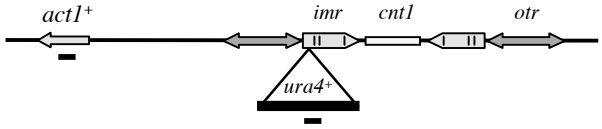

B

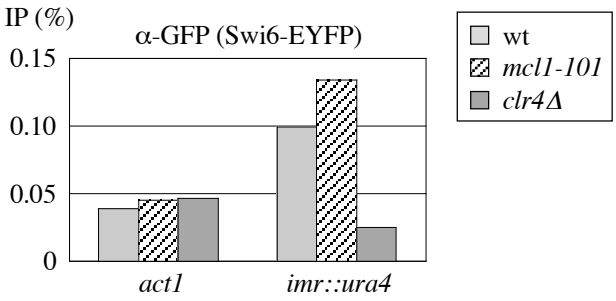

FIG. S2. Chromatin association of Swi6-EYFP at *imr::ura4*+. (A) Schematic diagrams of *S. pombe* chromosome and locations of PCR primers used in chromatin immunoprecipitation assay (horizontal line). (B) ChIP was performed using α-GFP antibody for cells carrying *imr::ura4*+ and expressing Swi6-EYFP in the wt (TN477), *mcl1-101* (TN479), and *clr4Δ* (TN490) background. Precipitated DNA was quantified by real-time PCR using LightCycler (Roche). The ratios of immunoprecipitated DNA to input DNA obtained from one repetition are shown. All strains were incubated at semi-permissive temperature for the *mcl1-101* (32 ºC)

A

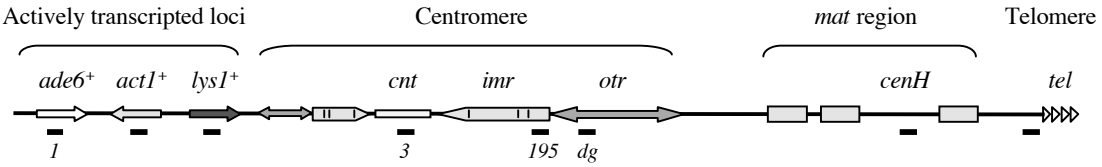

B

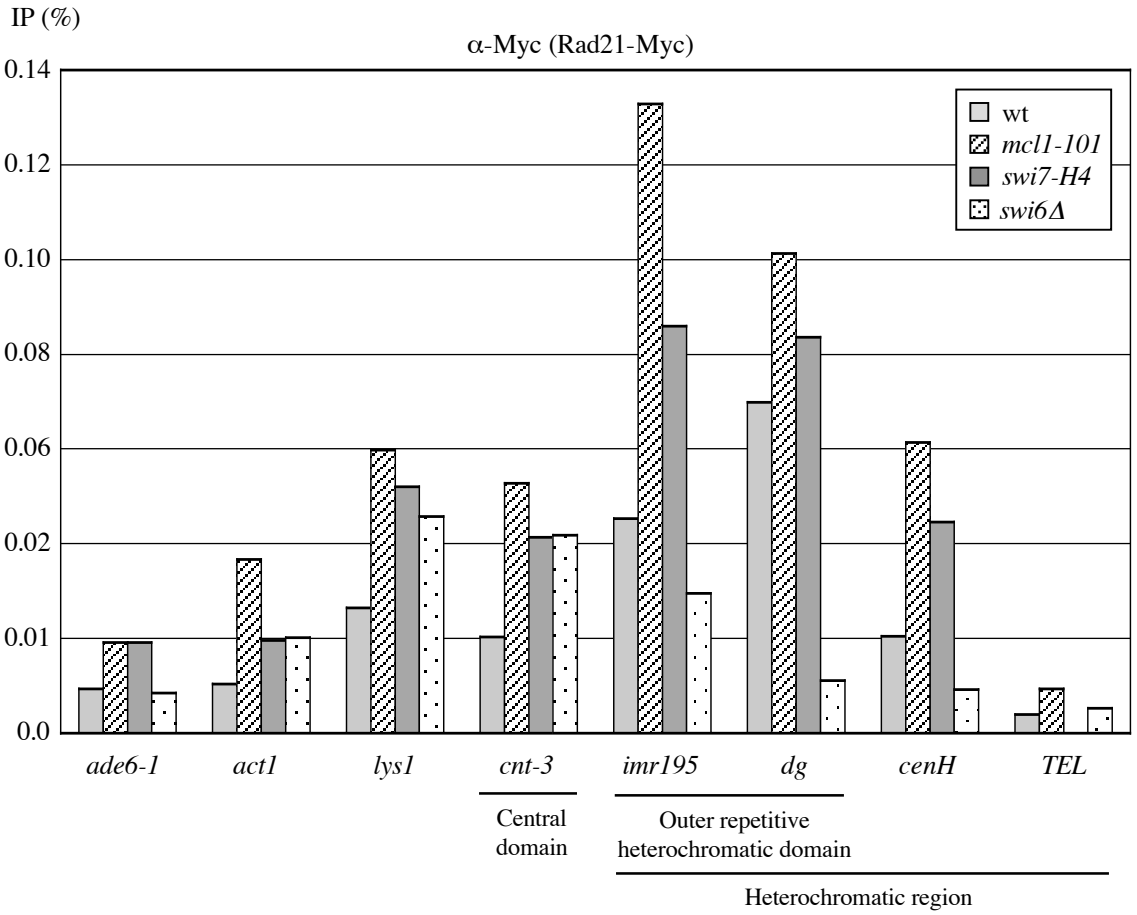

FIG. S3. Chromatin association of Rad21-Myc in the *mcl1-101* mutant. (A) Schematic diagram of *S. pombe* chromosome and locations of PCR primers used in chromatin immunoprecipitation assay (horizontal lines). (B) ChIP was performed using α-Myc antibody for cells expressing Rad21-Myc in the wt (TN658), *mcl1-101* (TN867), *swi7-H4* (TN889) and *clr4Δ* (TN870) background. Precipitated DNA was quantified by real-time PCR using LightCycler (Roche). The ratios of immunoprecipitated DNA to input DNA obtained from one repetition are shown. All strains were incubated for 6 hr at restrictive temperature for the *mcl1-101* (37 ºC).

A

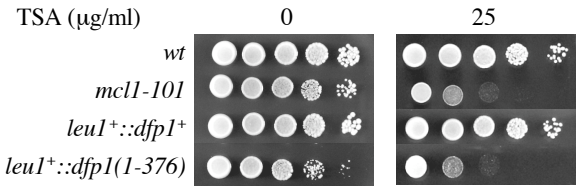

B *cnt1::ura4+*

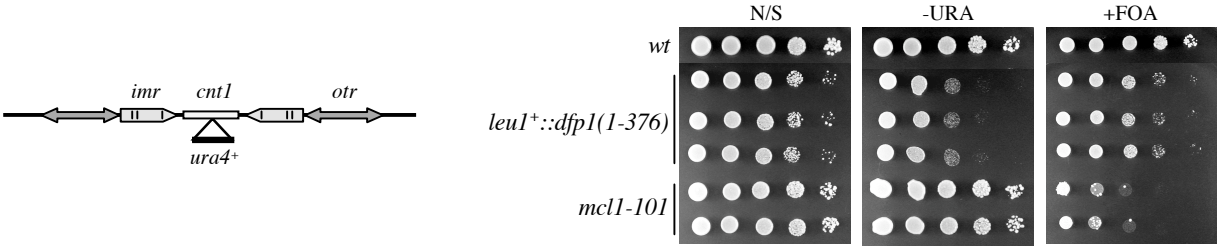

FIG. S4. The *dfp1* mutant is sensitive to TSA, but does not show alleviation of transcriptional gene silencing at the central domain. (A) Ten-fold serial dilutions of wt (JY746), *mcl1-101* (TN167), *leu1::dfp1*$^{+}$ (GBY572), *leu1::dfp1*$_{1\text{-}376}$ (AFY7) strains were plated onto YES containing indicated concentration of TSA and incubated at 30 ºC for 3 day. (B) Left: schematic diagram of the marker gene inserted at *cnt* of *cen1* (*cnt1*). Right: Ten-fold serial dilutions of wt (FY336), *leu1::dfp1*$_{1\text{-}376}$ (TN886–888), and *mcl1-101* (TN667, TN668) strains were plated onto non-selective EMM (N/S), EMM lacking uracil (-URA), EMM containing 5-FOA (FOA). Plates were incubated at 30 ºC for 4 days.

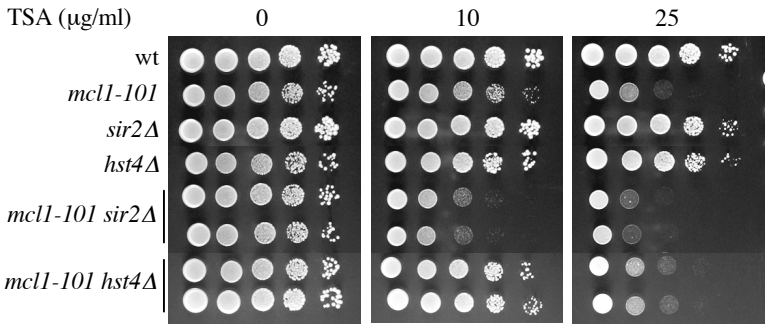

FIG. S5. Genetic interactions between Mcl1 and HDACs. (A) Ten-fold serial dilutions of wt (JY746), *mcl1-101* (TN167), *sir2Δ* (TN583), *hst4Δ* (TN582), *mcl1-101 sir2Δ* (TN639 and TN642), and *mcl1-101 hst4Δ* (TN633 and TN634) strains were plated onto YES containing indicated concentration of TSA and incubated at 30 ºC for 3 day.